Giant Star-shaped *meso*-substituted Fluorescent Porphyrins with Fluorenyl-containing Arms Designed for Two-photon Oxygen Photosensitization

Limiao Shi,[a] Zhipeng Sun,[a] Nicolas Richy,[a] Mireille Blanchard-Desce,[b] Olivier Mongin,[a] Frédéric Paul,[a] Christine Paul-Roth,[a,*]

Table of Contents:

1. Synthesis of the precursor **20** p. S3

2. ^{1}H NMR spectra of aldehydes **7**, **8**, **9**, **10**, **11**, and precursors **12**, **15**, **20** and **23** p. S4

3. Comparative ^{1}H NMR spectra of porphyrins **2a**, **6b-e** and **6b-d-Zn** p. S13

4.^{1}H NMR characterization of aldehyde precursors, free-bases and Zn(II) porphyrins and study of their thermal stability in solution p. S18

5. ^{13}C{^{1}H} NMR spectra of aldehydes **7**, **8**, **9**, **10** and **11** p. S27

6. ^{13}C{^{1}H} NMR spectra for porphyrins **2a**, **6b-e** and **6b-d-Zn** p. S32

7. Absorption and emission spectra of the aldehyde precursors **8-11** p. S37

8. Energy transfer efficiencies for **6b-e** and **6b-d-Zn** p. S39

9. Two-photon excited fluorescence (2PEF) data for **2a**, **6b-e** and **6b-d-Zn** p. S40

1. Synthesis of the precursor 20

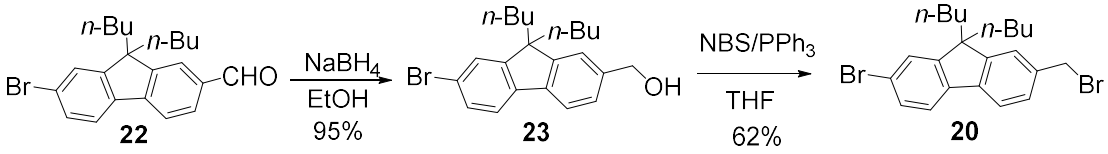

Scheme S1. Synthesis of **20**.

7-Bromo-9,9-dibutyl-9H-fluoren-2-yl)methanol (23). In a Schlenk tube, $NaBH_4$ (193 mg, 5.11 mmol, 1.2 eq) was added to a solution of 7-bromo-9,9-dibutyl-9*H*-fluorene-2-carbaldehyde **22**[1] (1.6 g, 4.26 mmol, 1 eq) in EtOH (30 mL) at 0 ºC under an argon stream. Stirring was kept at 0 ºC for 1 h. The solution was allowed to warm up to room temperature, and the reaction was stirred for another 2 h at room temperature. The mixture was extracted with EtOAc/water, after washed by brine. After evaporation of the solvent, the residue was further purified by chromatography (heptane/CH_2Cl_2 = 1/1, vol/vol), affording the title compound **23** as a white solid (1.6 g, 95%). ^{1}H NMR (300 MHz, $CDCl_3$, ppm): δ = 7.67 (t, *J* = 4.2 Hz, 1H), 7.56 (dd, *J* = 6.3, 2.4 Hz, 1H), 7.49-7.45 (m, 2H), 7.36-7.34 (m, 2H), 4.80 (s, 2H), 2.02-1.90 (m, 4H), 1.66 (s, 1H), 1.17-1.04 (m, 4H), 0.70 (t, *J* = 7.5 Hz, 6H), 0.66-0.55 (m, 4H).

2-Bromo-7-(bromomethyl)-9,9-dibutyl-9H-fluorene (20). In a Schlenk tube, NBS (758 mg, 4.26 mmol, 1.1 eq) was added to a solution of (7-bromo-9,9-dibutyl-9*H*-fluoren-2-yl)methanol **23** (1.5 g, 3.87 mmol, 1 eq) and PPh_3 (1.1 g, 4.26 mmol, 1.1 eq) in dry THF (30 mL) at 15 ºC under an argon stream. The mixture was stirred for 1h and immediately quenched with cold water. The mixture was extracted with CH_2Cl_2 and washed with brine. After evaporation of the solvent, the residue was further purified by chromatography (heptane/CH_2Cl_2 = 4/1, vol/vol), leading to the title compound as a white solid (1.1 g, 62%). ^{1}H NMR (300 MHz, $CDCl_3$, ppm): δ = 7.64 (d, *J* = 7.8 Hz, 1H), 7.58-7.55 (m, 1H), 7.50-7.46 (m, 2H), 7.40-7.34 (m, 2H), 4.62 (s, 2H), 2.04-1.88 (m, 4H), 1.16-1.05(m, 4H), 0.71 (t, *J* = 7.2 Hz, 6H), 0.65-0.54 (m, 4H).

[1] Yao, D.; Zhang, X.; Mongin, O.; Paul, F.; Paul-Roth, C. O.; *Chem. Eur. J.* **2016**, *22*, 5583-5597.

2. ^{1}H NMR spectra of aldehydes 7, 8, 9, 10, 11 and precursors 12, 15, 20 and 23

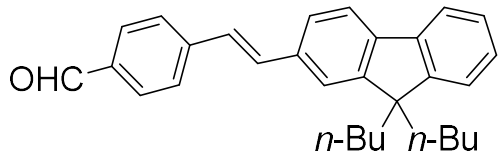

7

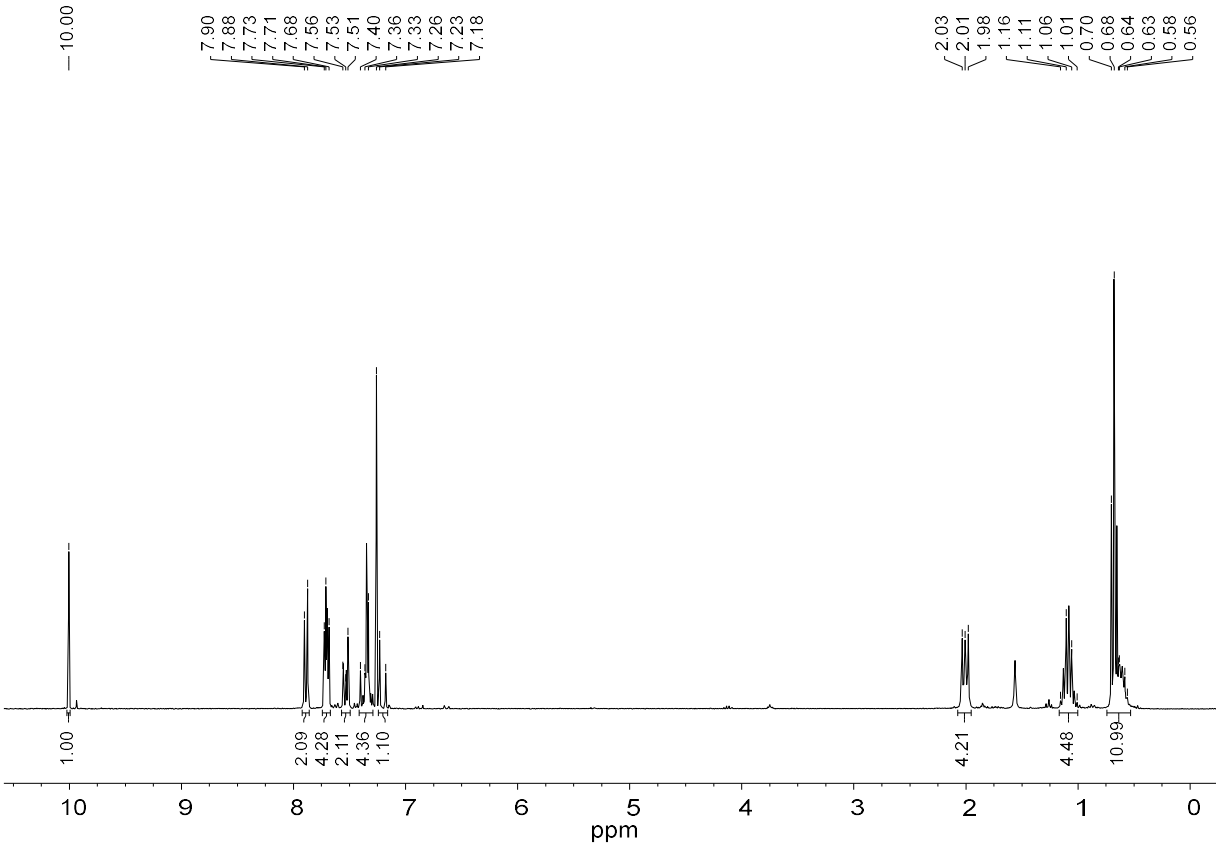

Figure S1. ^{1}H NMR spectrum at 300 MHz for **7** in $CDCl_3$.

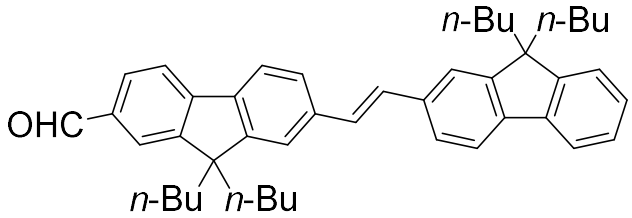

8

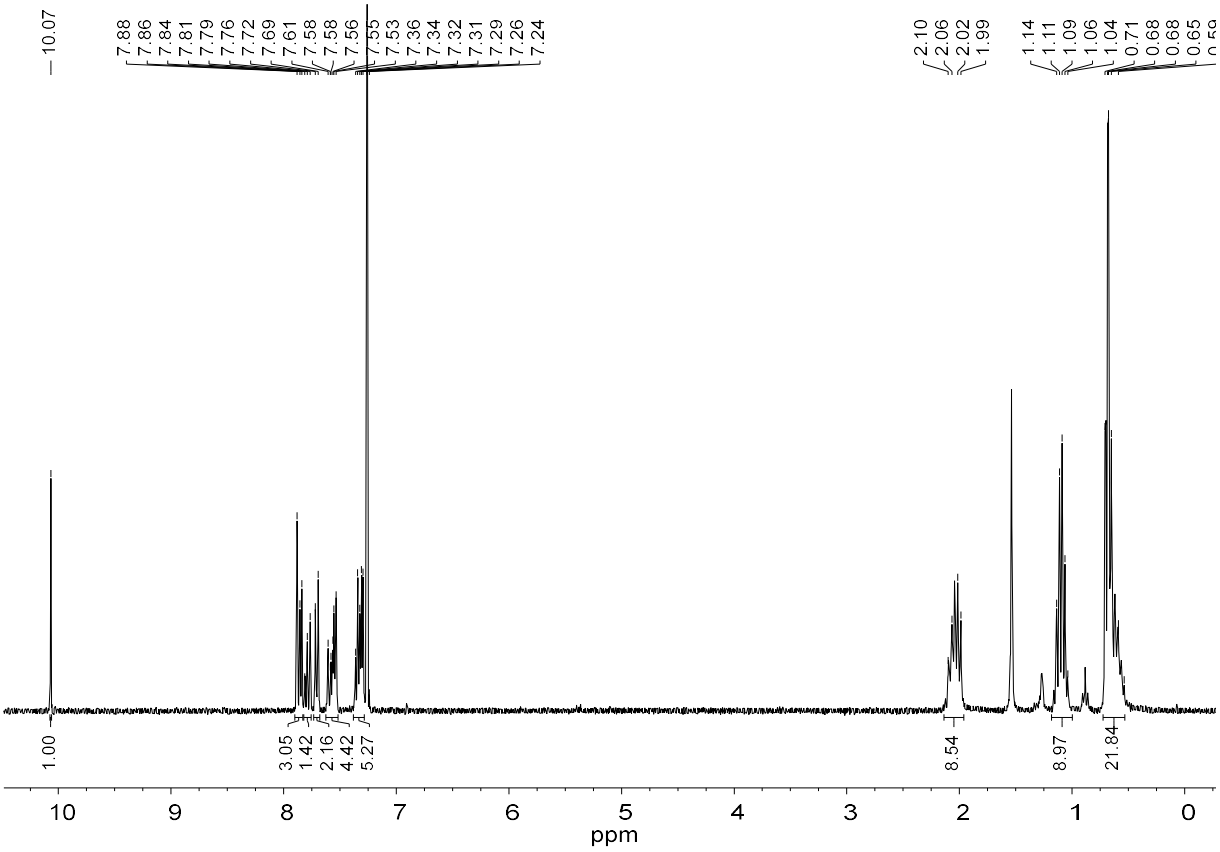

Figure S2. ^{1}H NMR spectrum at 300 MHz for **8** in $CDCl_3$.

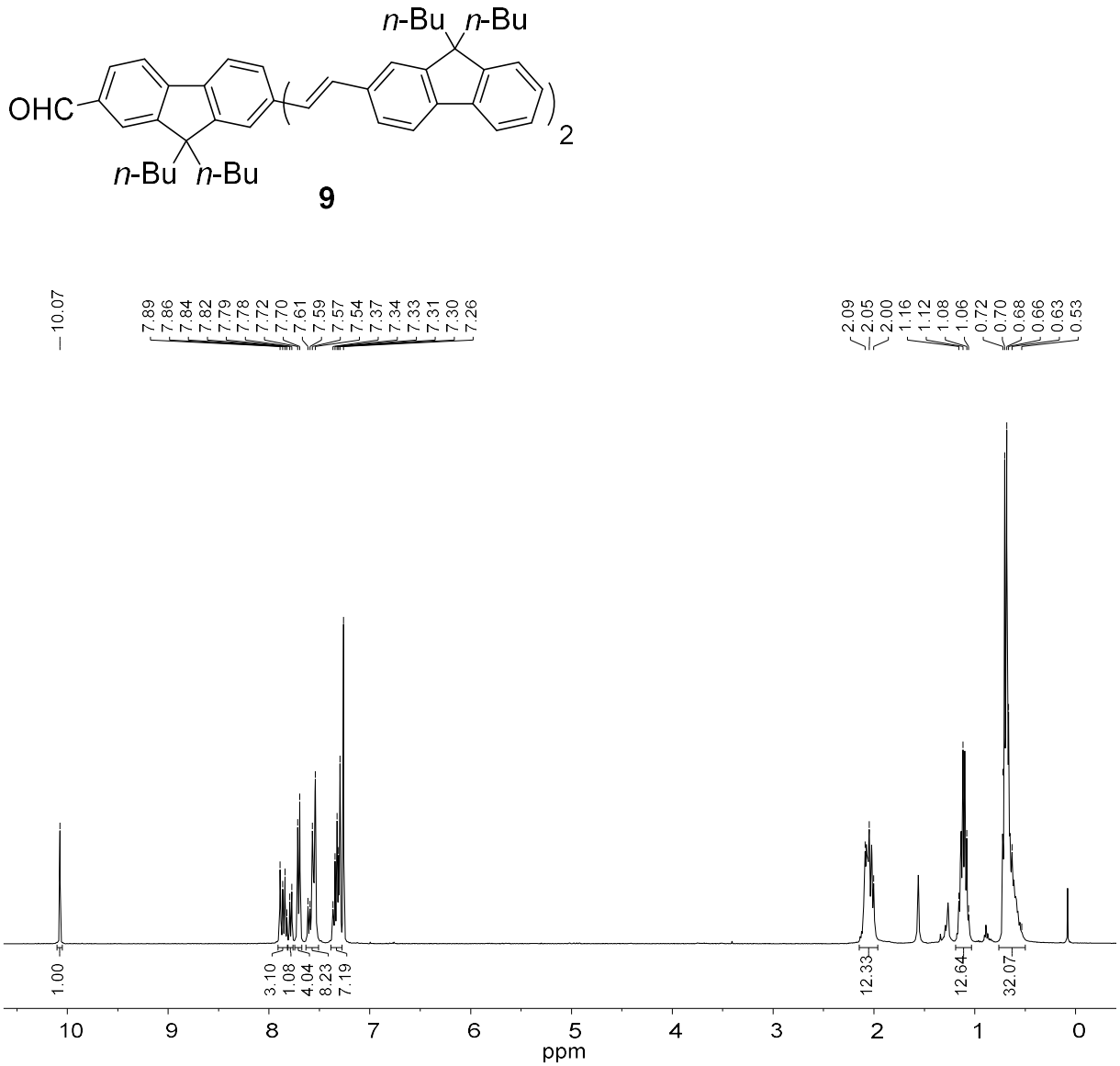

Figure S3. ^{1}H NMR spectrum at 300 MHz for **9** in $CDCl_3$.

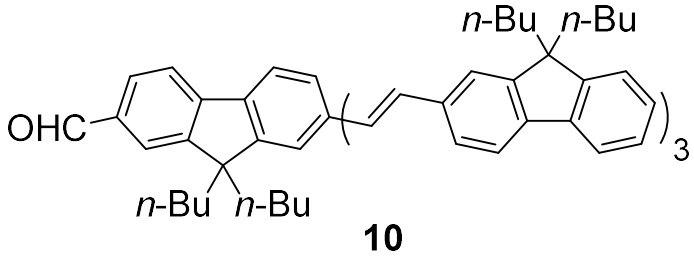

10

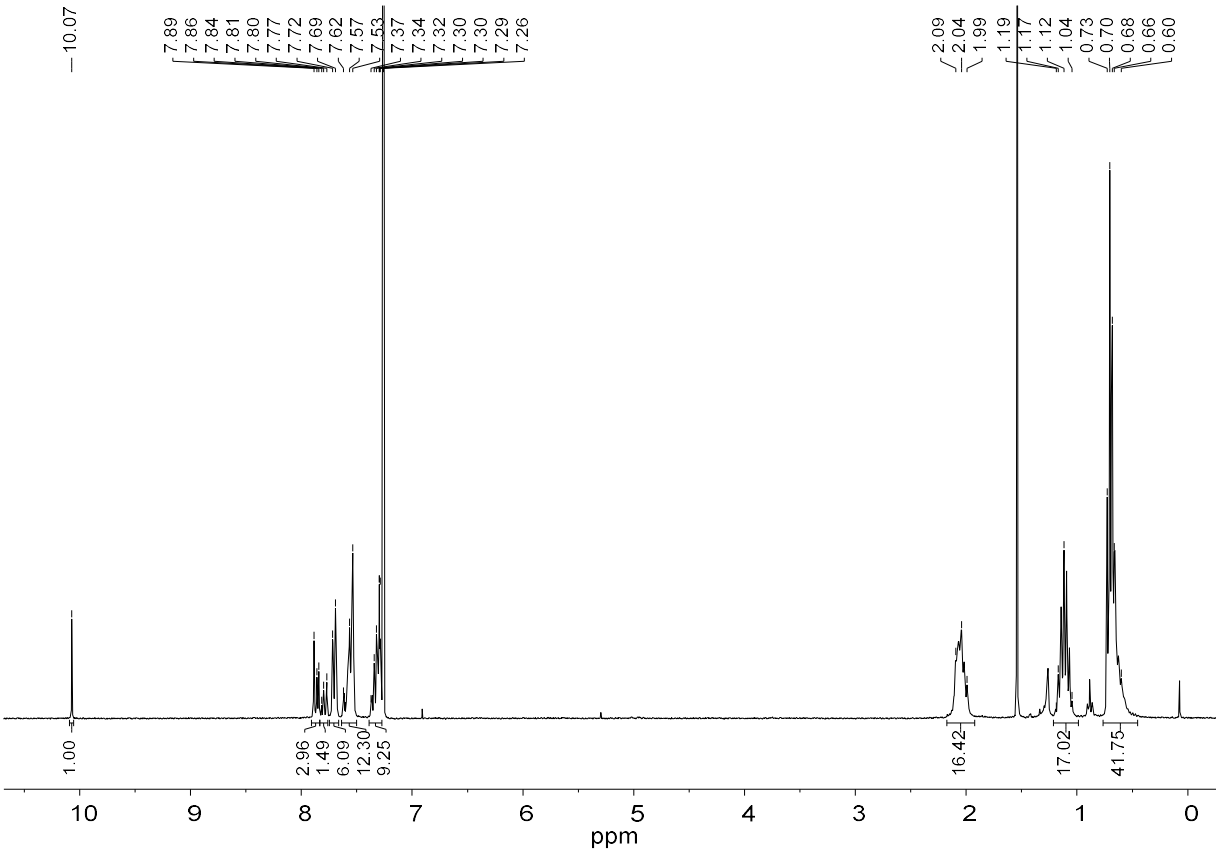

Figure S4. ^{1}H NMR spectrum at 300 MHz for **10** in $CDCl_3$.

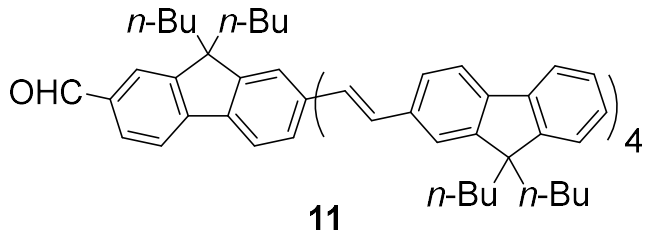

11

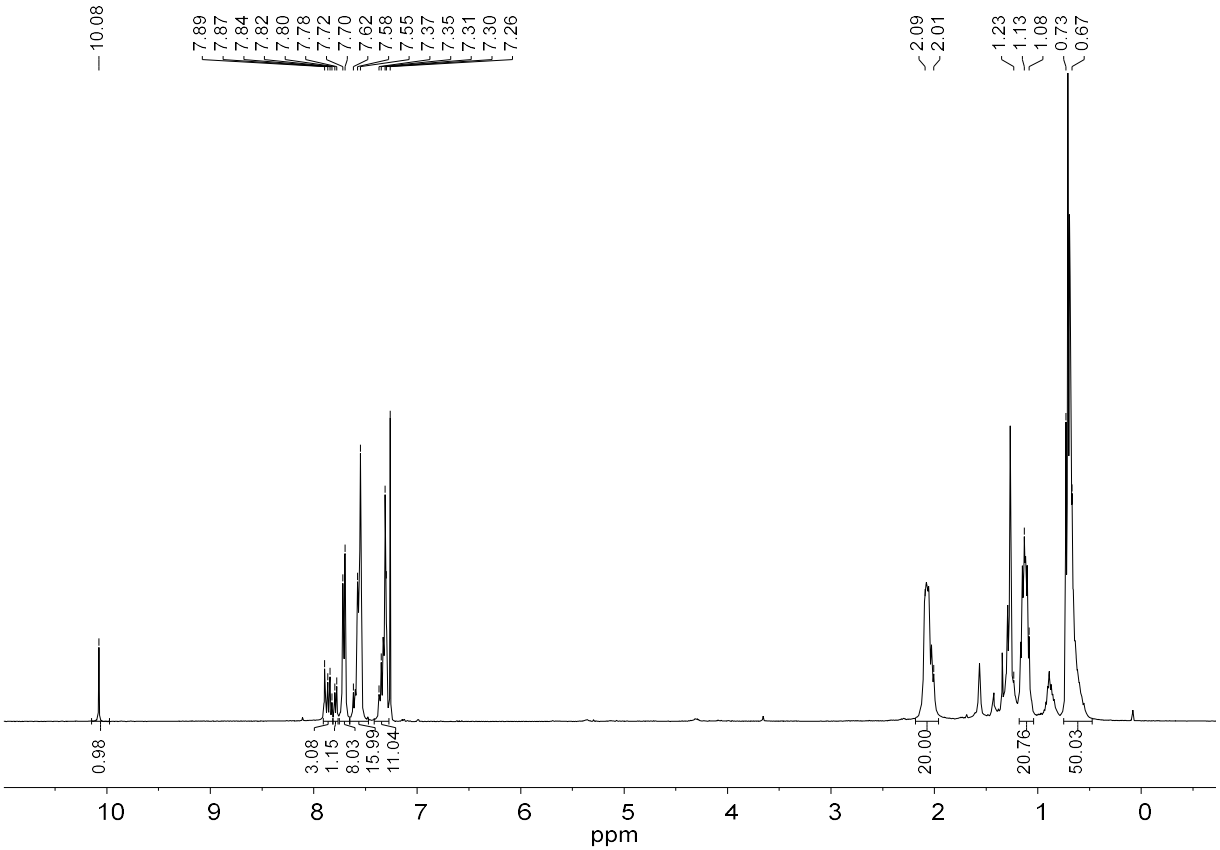

Figure S5. ^{1}H NMR spectrum at 400 for **11** in $CDCl_3$.

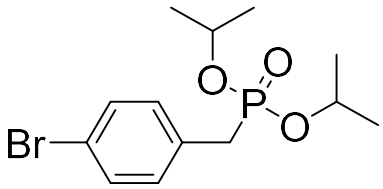

12

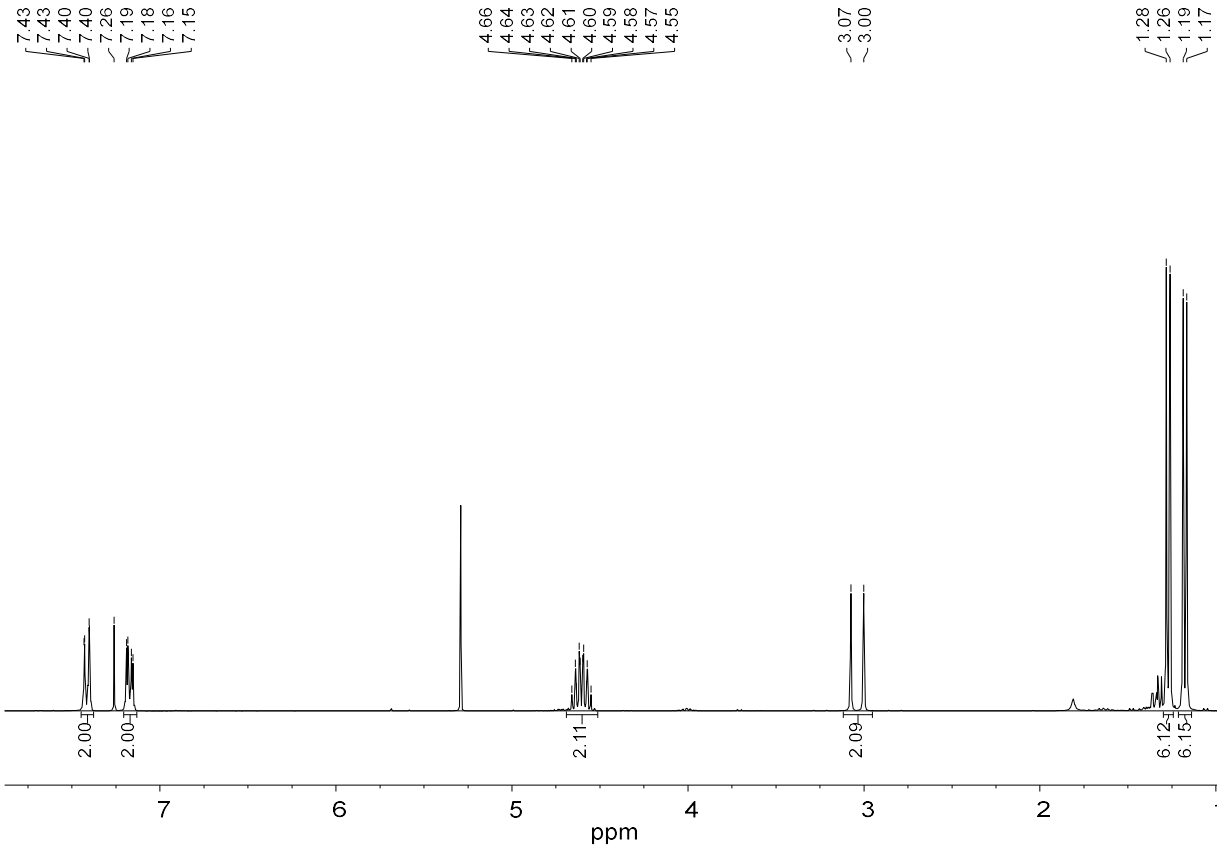

Figure S6. ^{1}H NMR spectrum at 300 MHz for **12** in $CDCl_3$.

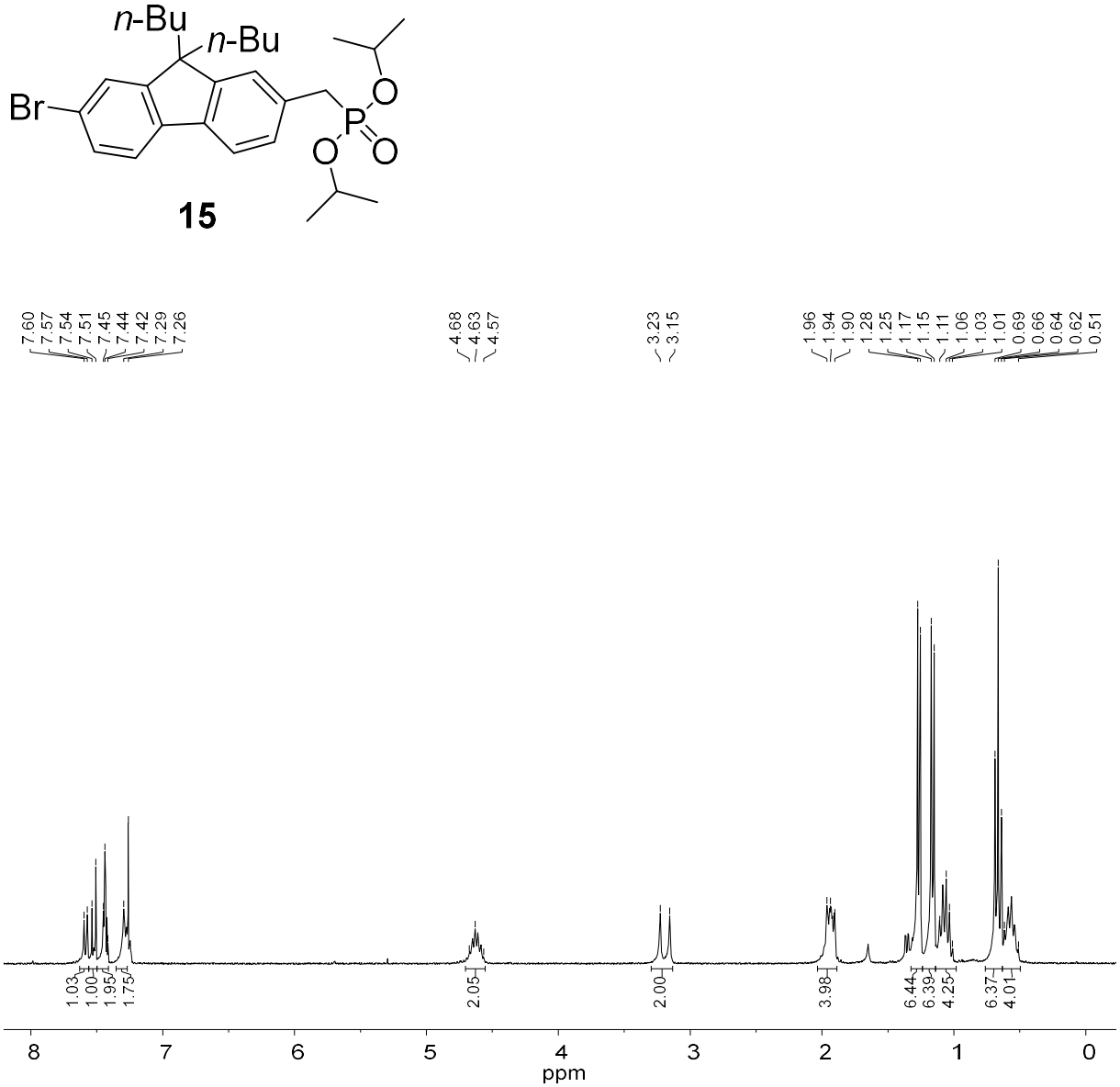

Figure S7. ^{1}H NMR spectrum at 300 MHz for **15** in $CDCl_3$.

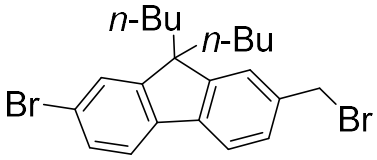

20

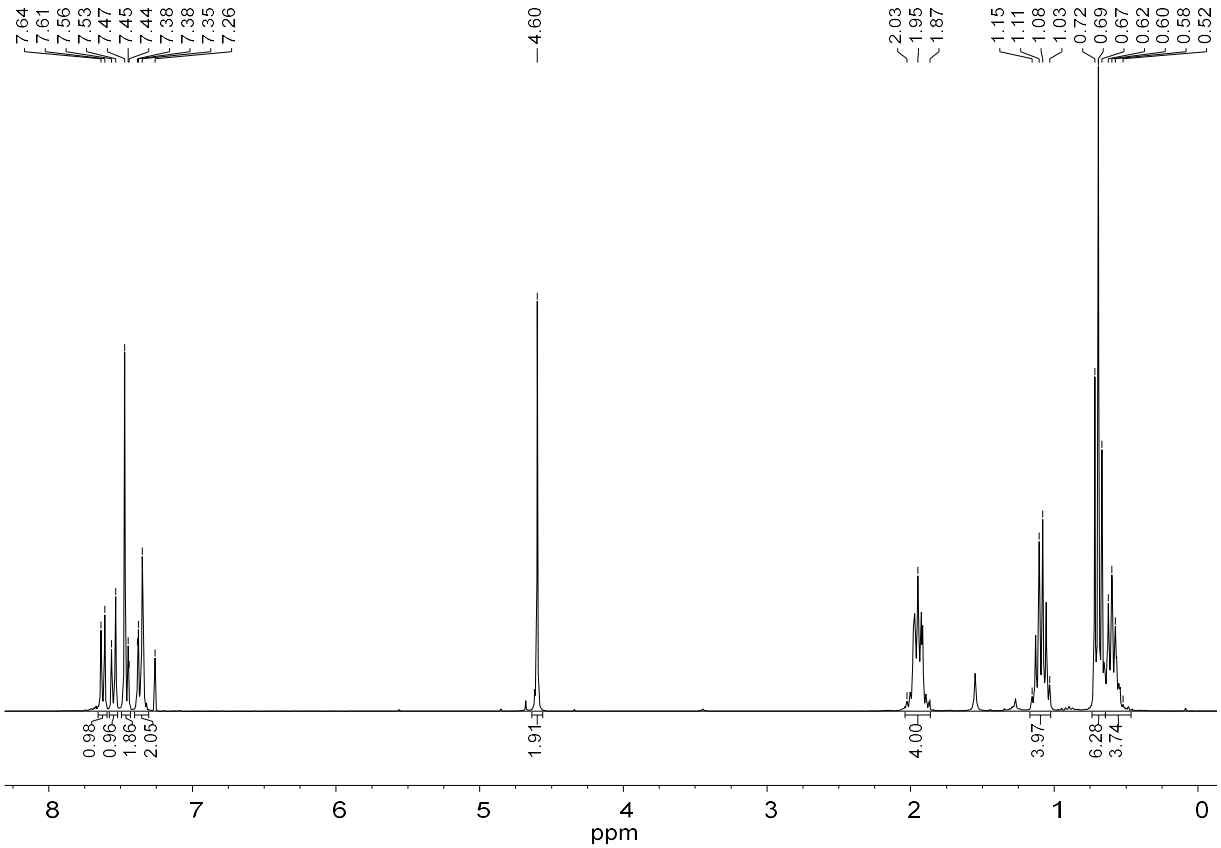

Figure S8. ^{1}H NMR spectrum at 300 MHz for **20** in $CDCl_3$.

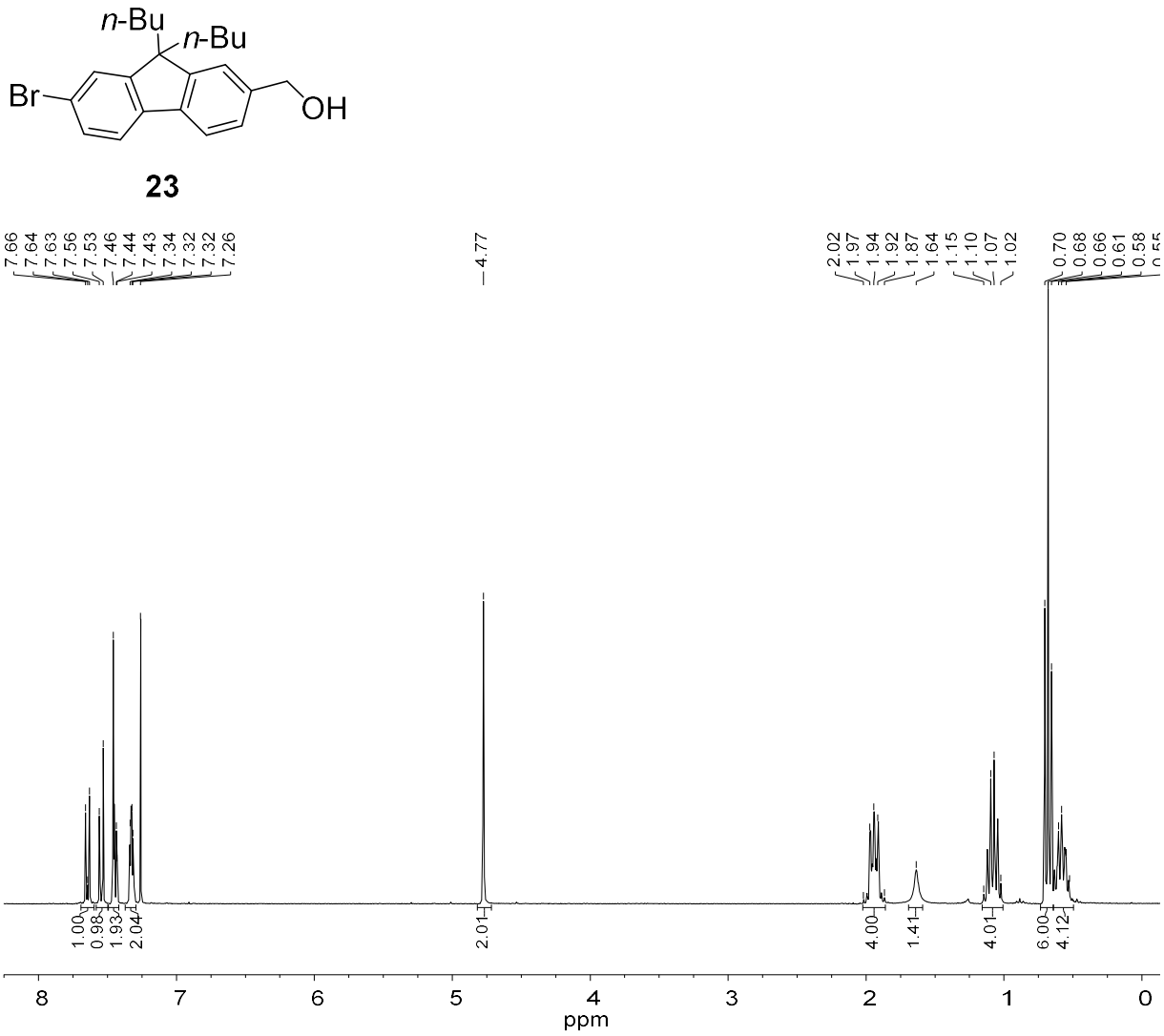

Figure S9. ^{1}H NMR spectrum at 300 MHz for **23** in $CDCl_3$.

3. Comparative ^{1}H NMR spectra of porphyrins 2a, 6b-e and 6b-d-Zn

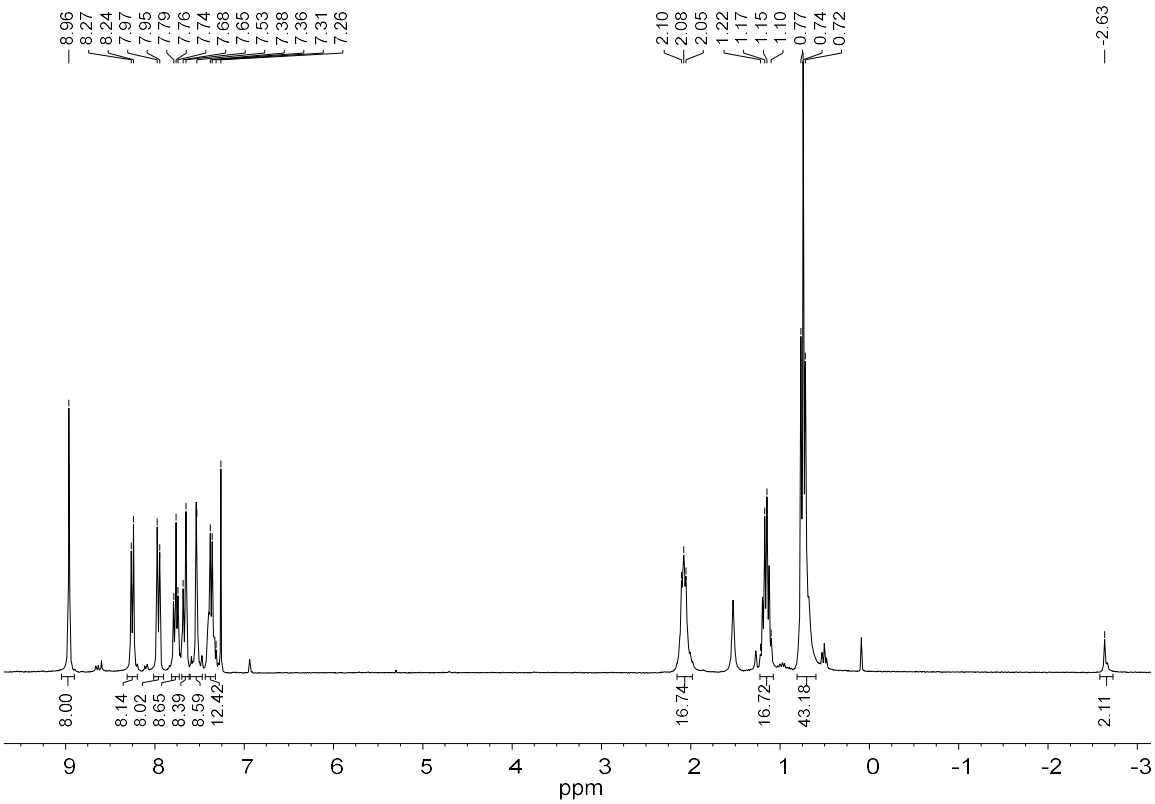

Figure S10. ^{1}H NMR spectrum at 300 MHz for **2a** in $CDCl_3$.

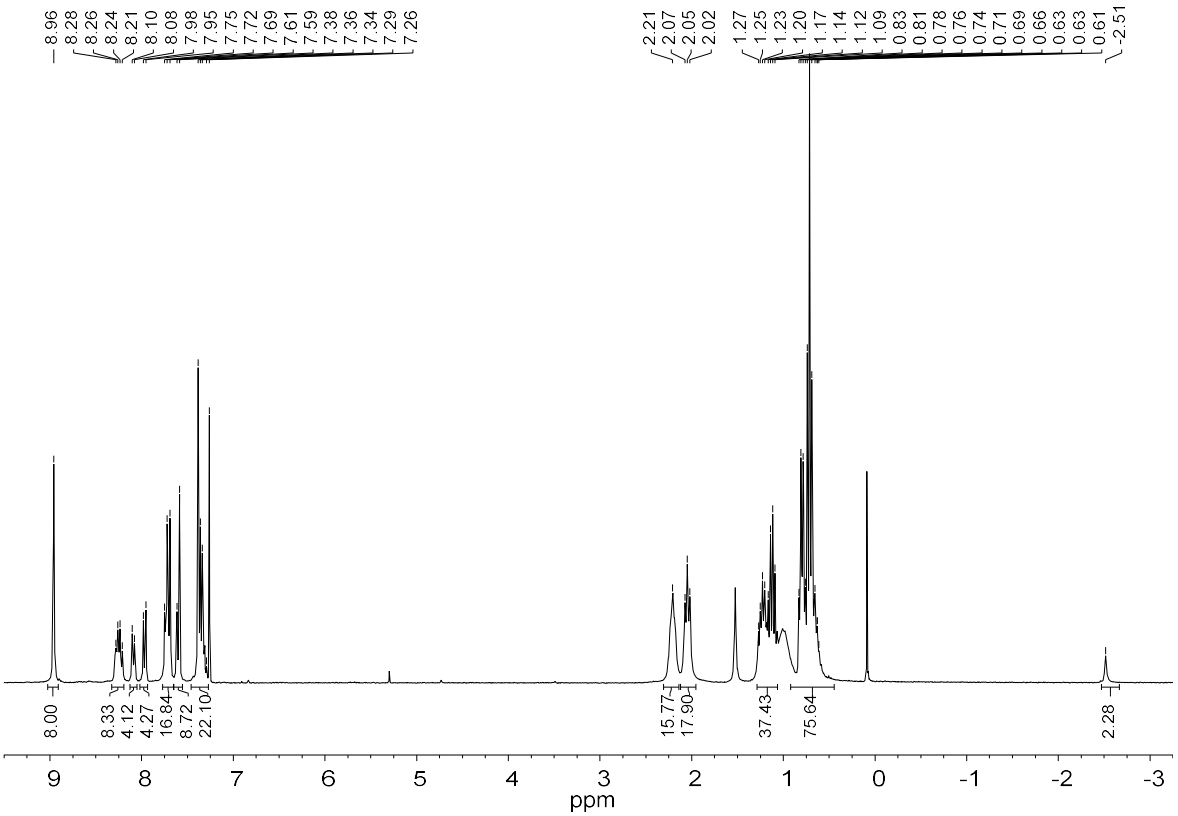

Figure S11. ^{1}H NMR spectrum at 300 MHz for **6b** in $CDCl_3$.

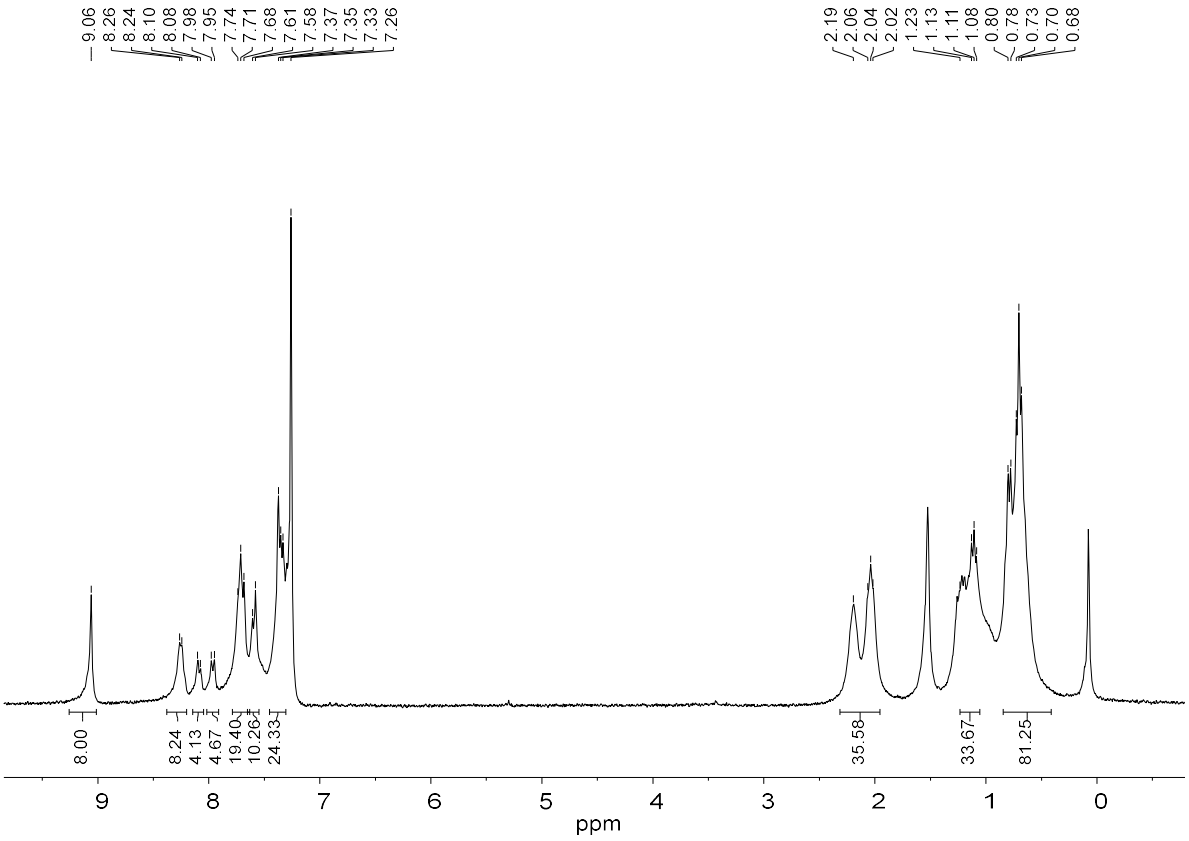

Figure S12. ^{1}H NMR spectrum at 300 MHz for **6b-Zn** in $CDCl_3$.

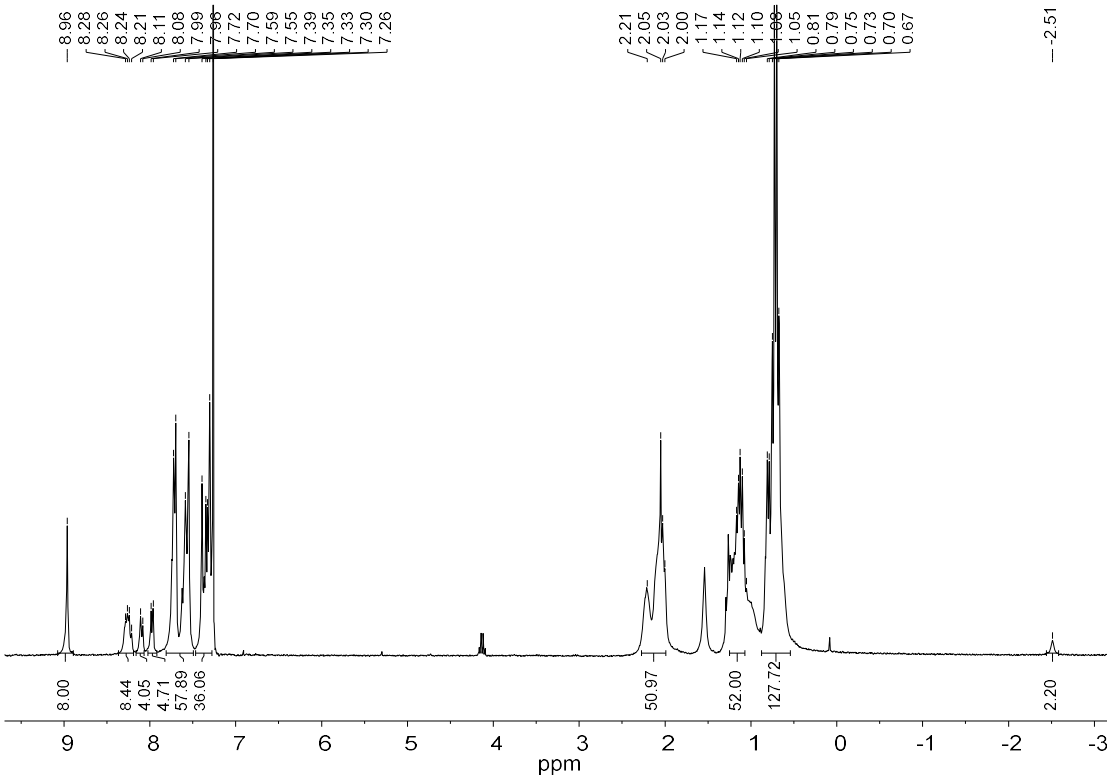

Figure S13. ^{1}H NMR spectrum at 300 MHz for **6c** in $CDCl_3$.

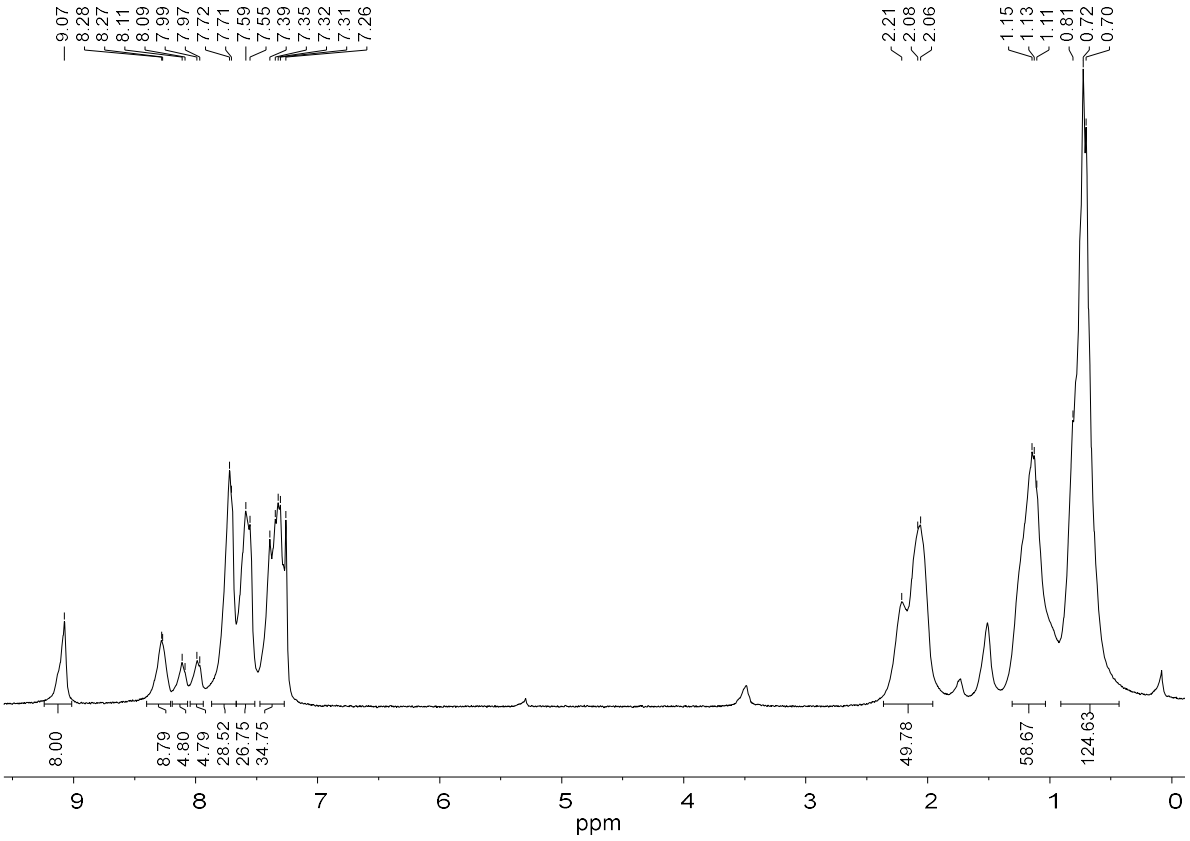

Figure S14. ^{1}H NMR spectrum at 300 MHz for **6c-Zn** in $CDCl_3$.

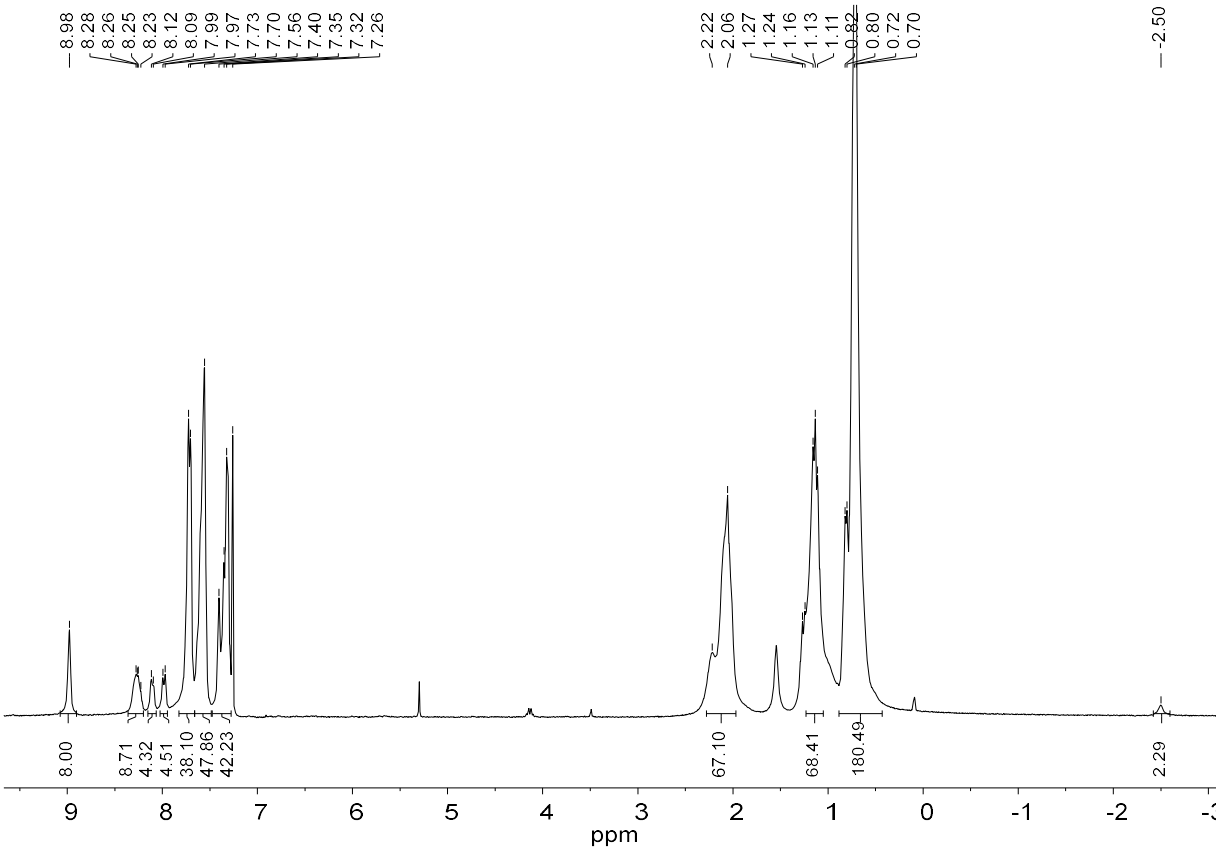

Figure S15. ^{1}H NMR spectrum at 300 MHz for **6d** in $CDCl_3$.

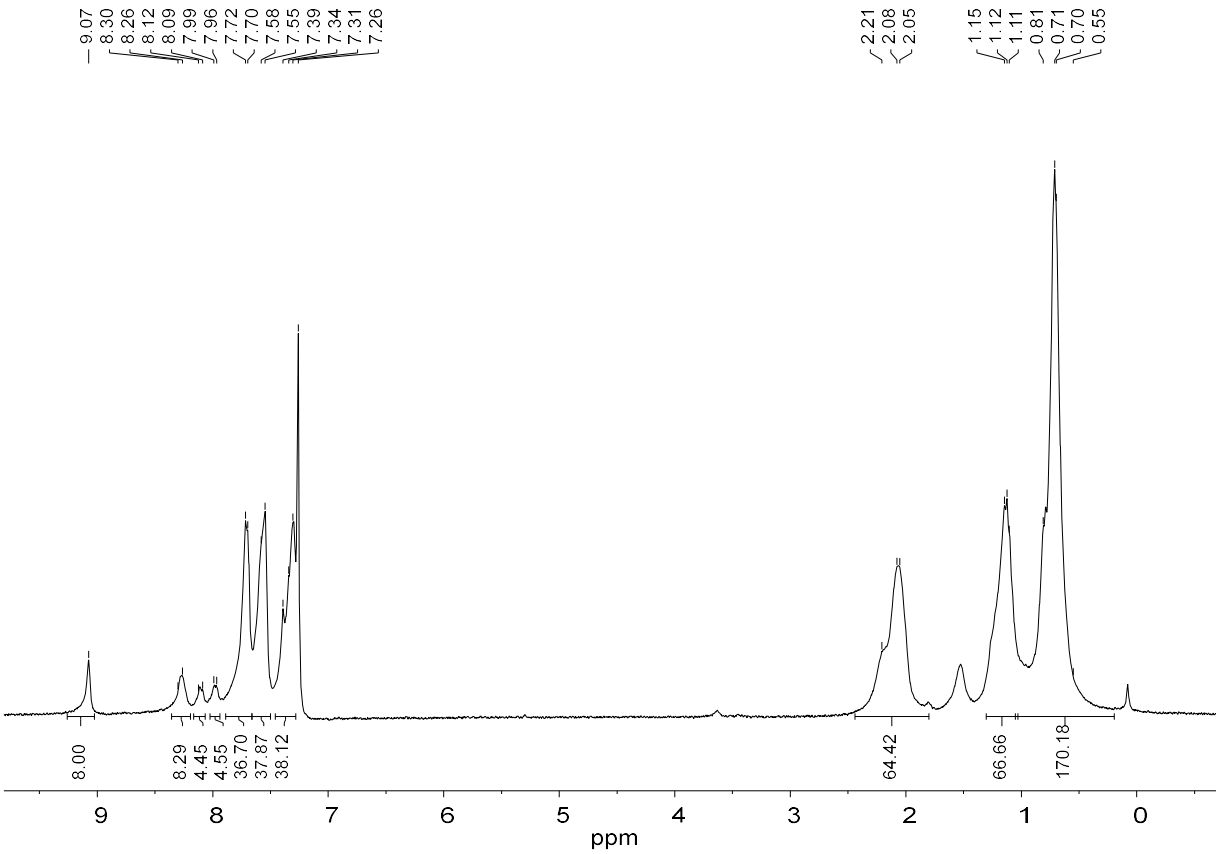

Figure S16. ^{1}H NMR spectrum at 300 MHz for **6d-Zn** in $CDCl_3$.

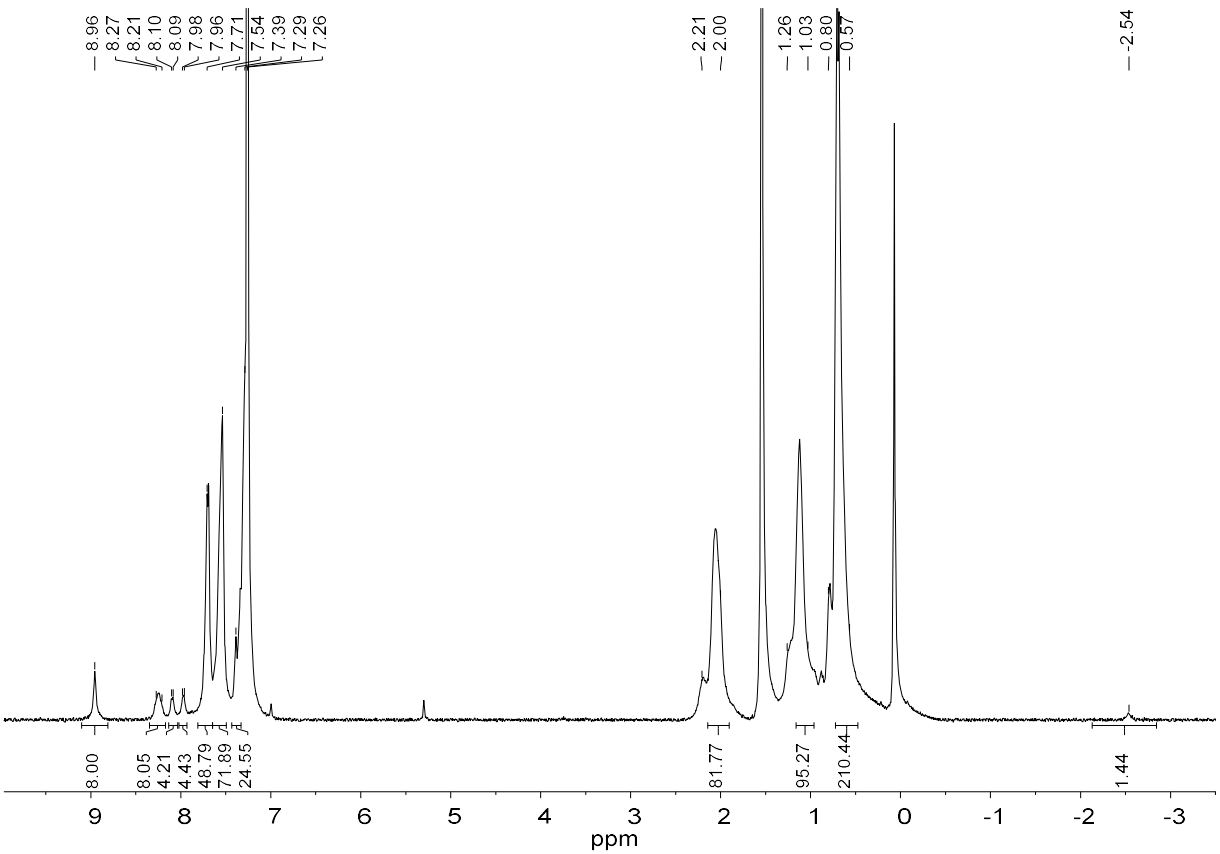

Figure S17. ^{1}H NMR spectrum at 400 MHz for **6e** in $CDCl_3$.

4. ^{1}H NMR characterization of aldehyde precursors, free-bases and Zn(II) porphyrins and study of their thermal stability in solution

Benzaldehyde 7: The ^{1}H NMR spectrum of this compound (Figure S18) presents three diagnostic signatures: (i) the aldehyde proton around 10 ppm, (ii) the aromatic protons of the phenyl and fluorenyl groups, around 7-8 ppm and (iii) the alkyl protons of the two butyl chains around 0-2 ppm. In the aromatic region, we can distinguish a doublet at 7.20 ppm with a coupling constant ^3J = 16 Hz, characteristic of the desired *E* configuration of the double bond.[2]

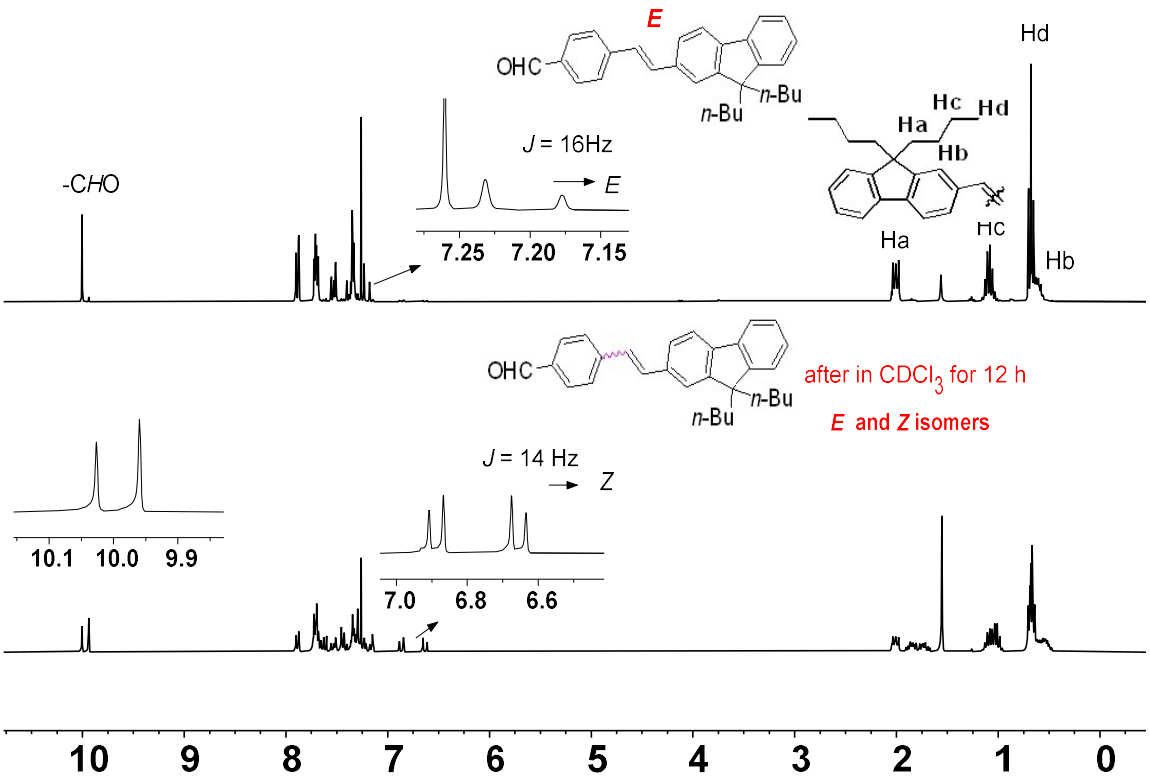

Figure S18. Detailed ^{1}H NMR spectra for the *E* stereoisomer of benzaldehyde **7** in $CDCl_3$ (top) and *E/Z* isomeric mixture obtained after 12 h (bottom).

[2] Yao, D.;. Zhang, X.; Abid, S.; Shi, L.; Blanchard-Desce, M.; Mongin, O.; Paul, F.; Paul-Roth, C. O.; *New J. Chem.*, **2018**, *42*, 395-401.

Stereochemical stability of 7 in solution: The stability of **7** was studied by ^{1}H NMR in $CDCl_3$. After 12 hours we observe (Figure S18) a new peak at around 10 ppm corresponding to a different aldehyde proton, and another doublet around 6.8 ppm. This last one presents a smaller coupling constant of ^{3}J = 14 Hz that is typical of a *Z* configuration of the double bond. We also notice that the *n*-butyl chain multiplets are shifted to higher field. We can conclude that *E* configuration of **7** is not stable in $CDCl_3$ solution over a few hours.

Benzaldehydes 8-11: Next, a comparison of the detailed ^{1}H NMR spectra of fluorenaldehyde*s* **8**, **9**, **10** and **11** is shown in Figure S19. As seen before for benzaldehyde **7**, the ^{1}H NMR spectra of all of these compounds present three parts: (i) a singlet for the aldehyde proton at around 10 ppm, (ii) the fluorenyl protons around 7-8 ppm, (iii) the alkyl protons of the *n*-butyl chains around 0-2 ppm. Comparing the protons belonging to the various fluorenyl groups around 7-8 ppm of aldehydes, **8**, **9**, **10** and **11** reveals that the intensity of the signal of the protons of the aldehyde function decreases in the expected proportions relative to those of the others protons of these molecules. In the case of fluorenaldehyde **9**, likewise to **7**, we can identify a doublet at 7.22 ppm with a coupling constant ^{3}J = 16 Hz, characteristic of the *E*-configuration.

Stereochemical stability of 8-11 in solution: We also monitored the stereochemical stability of these different aldehydes in solution by ^{1}H NMR, but no new peaks corresponding to a *Z*-vinyl proton appeared after 12 h. We conclude that the all-*E* isomers of all these fluorenaldehydes are thermally stable in $CDCl_3$ solutions.

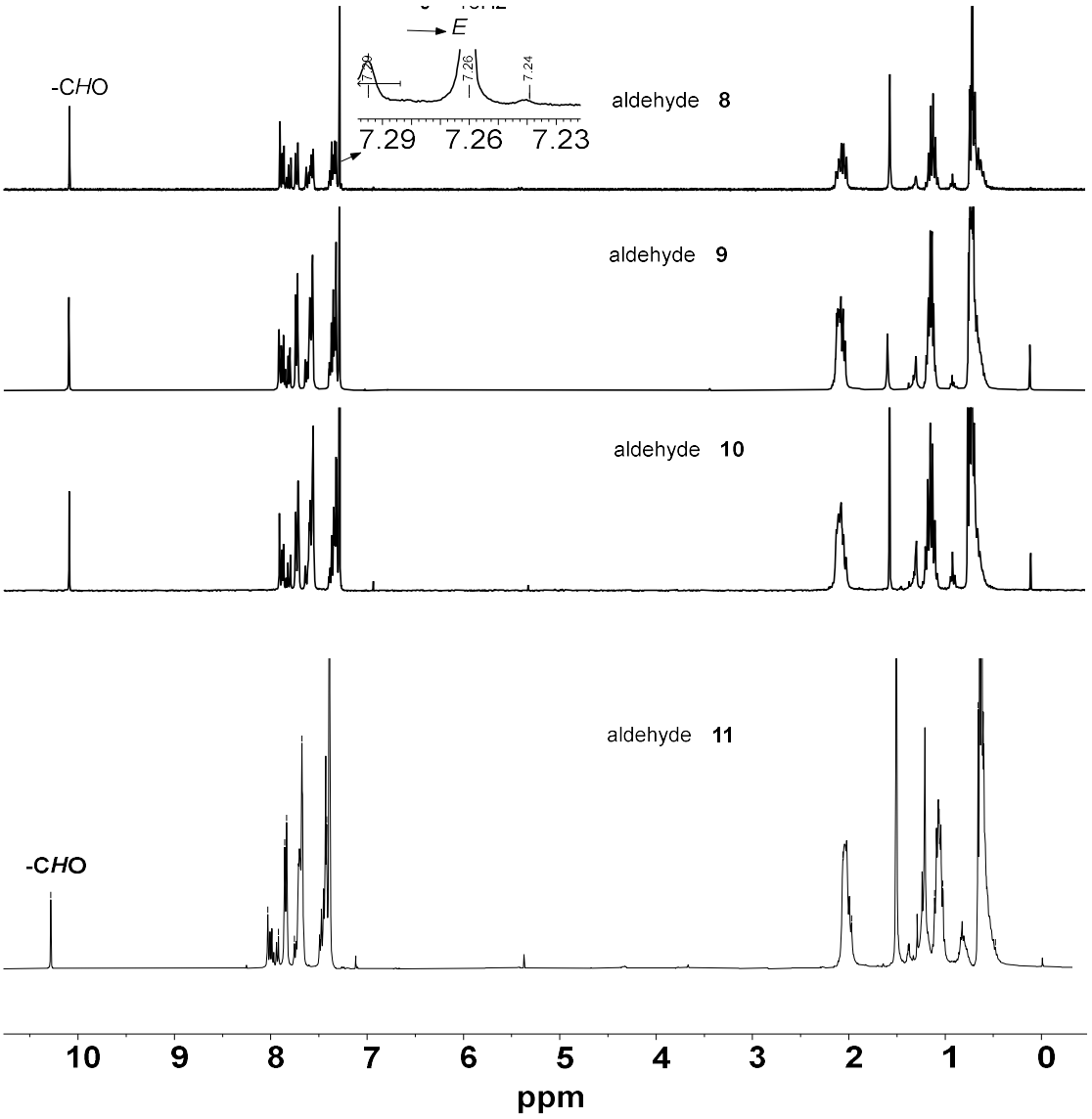

Figure S19. Complete ^{1}H NMR spectra of fluorenaldehydes **8**, **9**, **10** and **11** in $CDCl_3$.

Free-base porphyrin 2a: The full ^{1}H NMR spectrum of new **2a** is shown in Figure S20. We can easily detect the protons belonging to the porphyrin macrocycle: two –N*H* protons (singlet) in the shielding cone, at high field (-2.63 ppm) and eight β pyrrolic protons (H_β, singlet) at low field (8.96 ppm). Otherwise signals around 7.3-8.3 ppm (integrating for 44 protons) are detected: they belong to the protons of the phenyl and the fluorenyl groups. Furthermore, four groups of broad multiplets $H_{a,b,c,d}$ around 0.5 - 2.5 ppm, which integrate for 72 protons, are assigned to the butyl

chains of the four fluorenyl groups. At high field, we can also distinguish the two doublets of H_A and H_B for *para*-substituted phenyl groups at 8.24 ppm and 7.95 ppm, respectively.

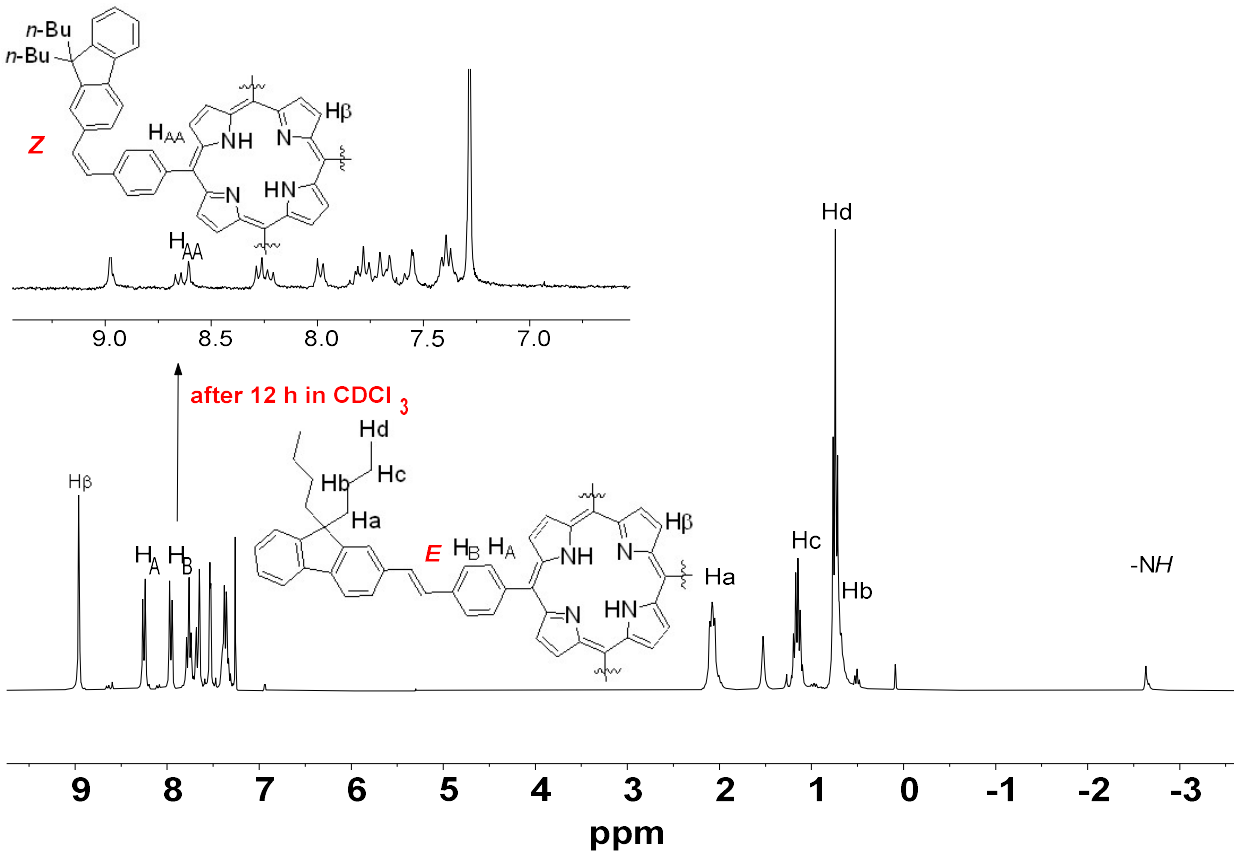

Figure S20. Detailed ^{1}H NMR spectra of *E/Z* stereoisomeric mixture of **2a** in $CDCl_3$.

Stereochemical stability of 2a: We monitored the stereochemical stability of this **TPP**-cored porphyrin in solution by ^{1}H NMR studies and observed appearance of other peaks around 8.5 ppm after 12 hours in $CDCl_3$. These are consistent with vinyl protons having a *Z* configuration. Obviously, likewise to its aldehyde precursor **7**, this all-*E* isomer is not configurationally stable in solution. The presence of *Z* double bonds is easily detected because we also observe new signals corresponding to H_{AA} protons of the phenyl groups shifted to lower field (8.5 ppm).

TFP-cored free-bases and Zn(II) complexes 6b-e and 6b-d-Zn: The ^{1}H NMR spectra of the **TFP**-cored derivatives **6b-e/6b-d-Zn** show four diagnostic signatures (Figure S21). For clarity, we will present the detail of these in two parts: (i) low field region (from 9.3 to 7.0 ppm) and (ii) high field region (from 2.5 to -3.5 ppm).

In the low field region, the partial ^{1}H NMR spectra (Figure S22) reveal: (a) the eight H_{β} protons around 9 ppm, with this singlet being shifted to lower field for zinc complexes with respect to free-base porphyrins (going from 8.9 to 9.1 ppm) (b) three peaks ($H_{A,B,C}$) around 7.9-8.3 ppm belonging to the four distinct aromatic protons of the *meso*-fluorenyl spacers and integrating in total for sixteen protons, well separated from the remaining aromatic protons of the peripheral fluorenyl groups around 7.3-7.8 ppm.

In the second, the high field region, the partial ^{1}H NMR spectra (Figure S23) reveal: (a) two –NH protons around -2.5 ppm (these appear for the free base porphyrins only, being replaced by a Zn(II) ion in the zinc porphyrin complexes **6b-Zn**, **6c-Zn** and **6d-Zn**), and (b) broad multiplets corresponding to the alkyl protons of the two distinct *n*-butyl chains. For the first compounds of this series, *i.e.* the TFP-cored porphyrins having only one extra fluorenyl unit on each arm (compound **6b** and its zinc complex **6b-Zn**), we observe two multiplets (at 2.0 and 2.2 ppm) integrating for sixteen protons each. As expected, as the length of the fluorenyl arm increases, the multiplet at higher field grows proportionally to the integrated protons.

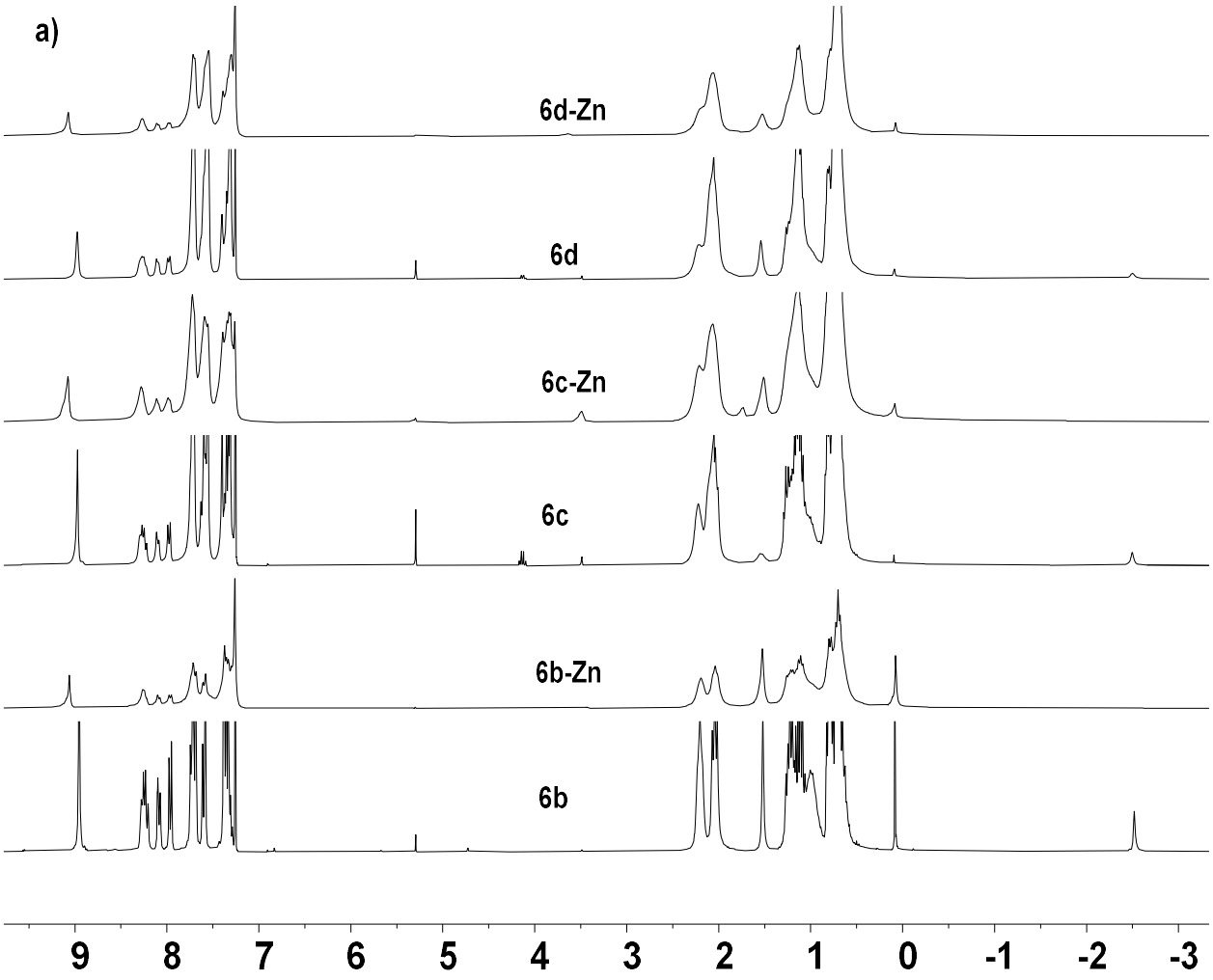

Figure S21. Complete ^{1}H NMR spectra of **TFP**-cored porphyrin series **6b-d** and **6b-d-Zn** in $CDCl_3$

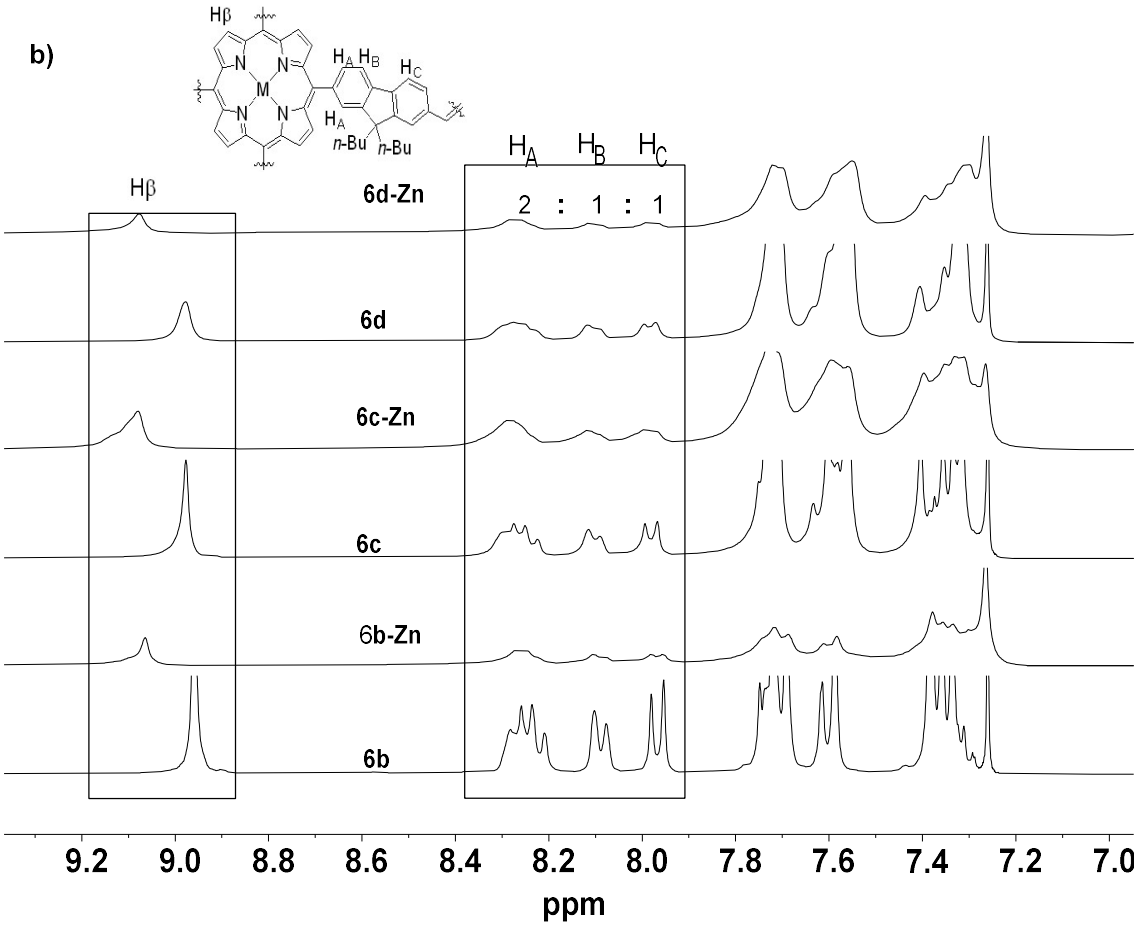

Figure S22. Partial ^{1}H NMR spectra (expansion) of previous series (low field region).

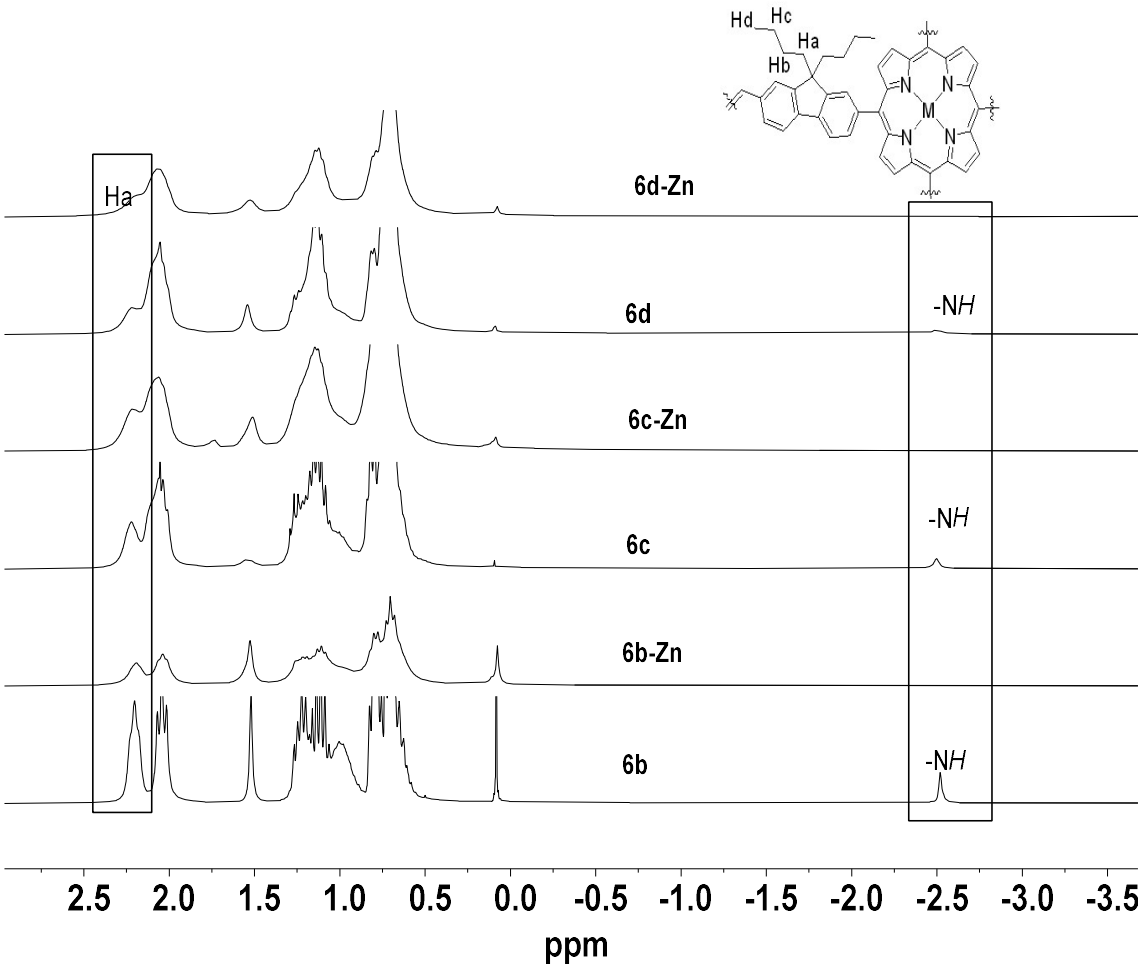

Figure S23. Partial ^{1}H NMR spectra (expansion) of previous series (high field region).

The complete ^{1}H NMR spectra of the largest free-base derivatives **6e** also shows these diagnostic signatures (Figure S24): (i) the β-pyrrolic protons of the porphyrin core (H_β) around 9 ppm, (ii) the aromatic protons around 7.2-8.5 ppm, (iii) the alkyl protons of the various butyl chains around 0.5-2.2 ppm and (iv) the two –NH protons within the porphyrin cavity around -2.5 ppm.

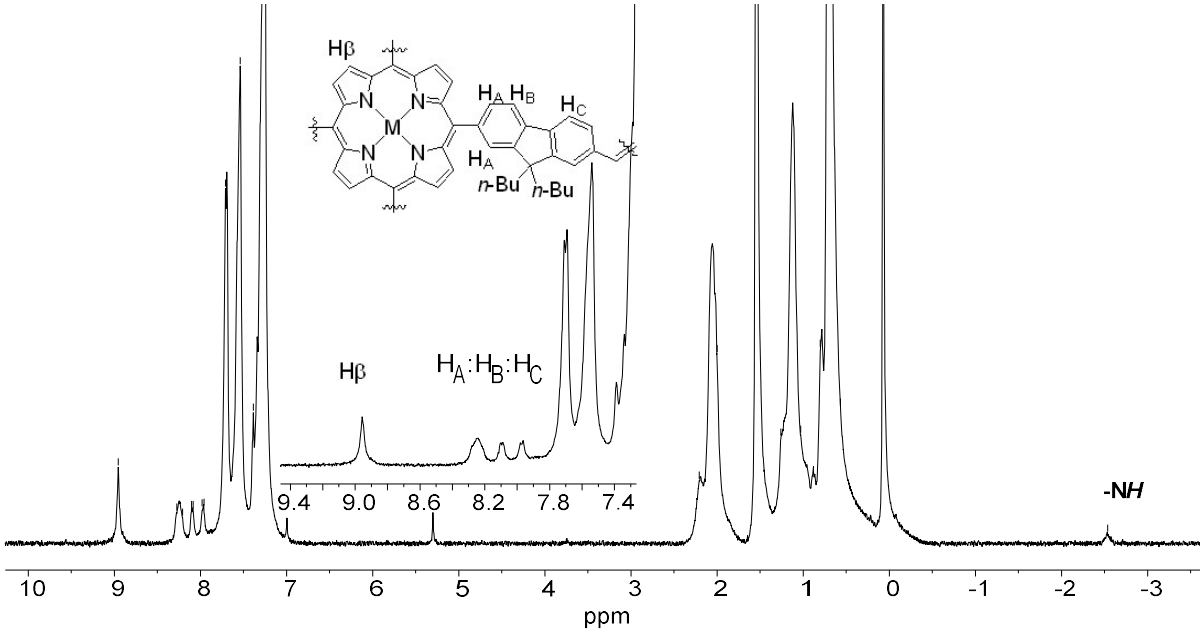

Figure S24. Complete ^{1}H NMR spectra of **6e** in $CDCl_3$.

5. $^{13}C\{^{1}H\}$ NMR spectra of aldehydes 7, 8, 9, 10 and 11

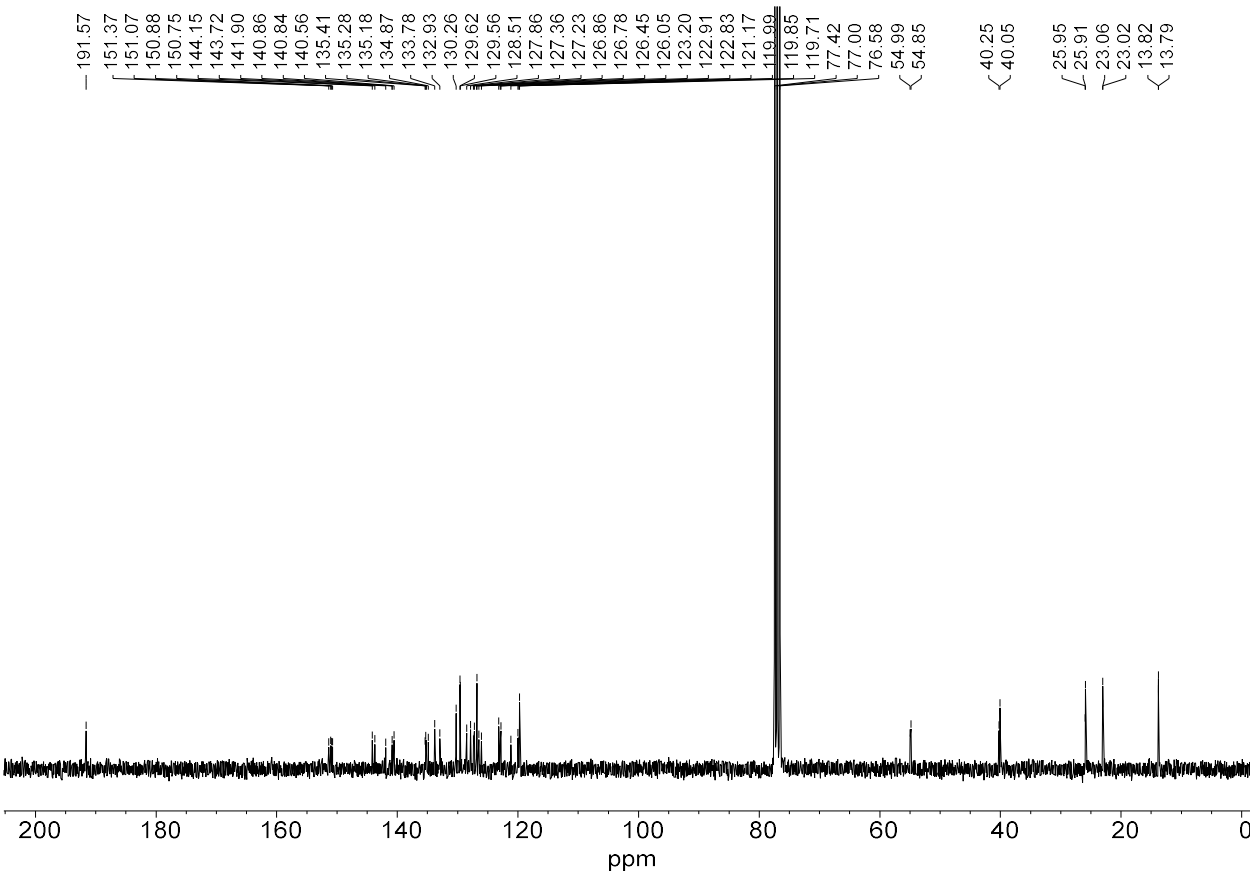

Figure S25. $^{13}C\{^{1}H\}$ NMR spectrum at 75 MHz for **7** in $CDCl_3$.

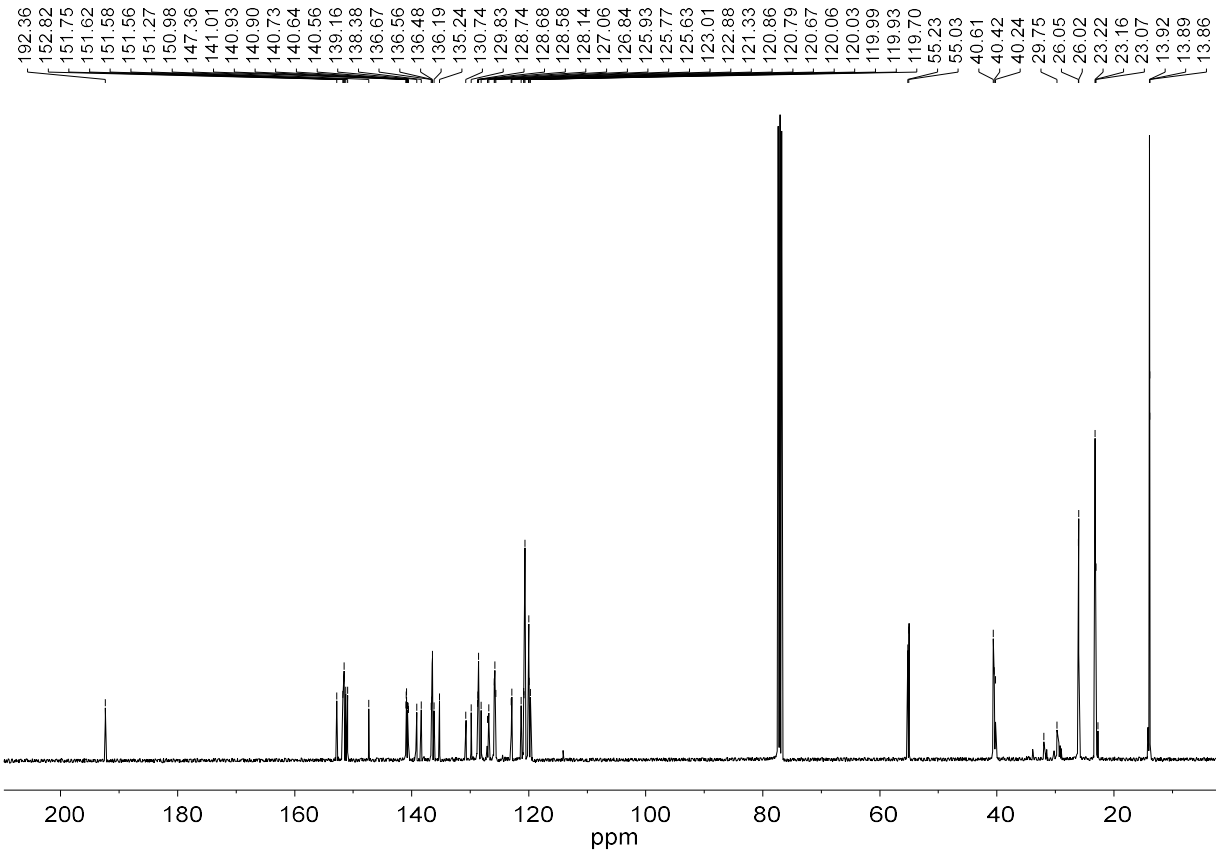

Figure S26. $^{13}C\{^{1}H\}$ NMR spectrum at 75 MHz for **8** in $CDCl_3$.

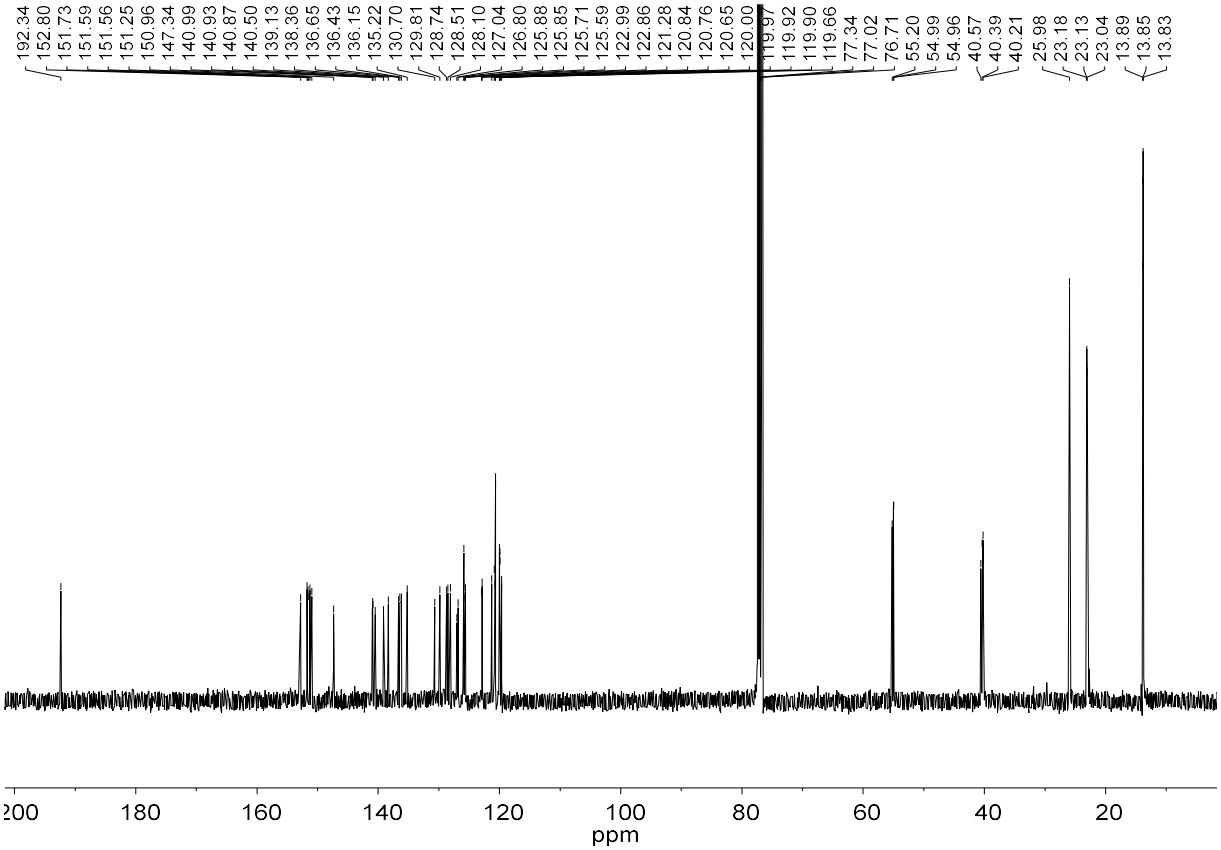

Figure S27. $^{13}C\{^{1}H\}$ NMR spectrum at 100 MHz for **9** in $CDCl_3$.

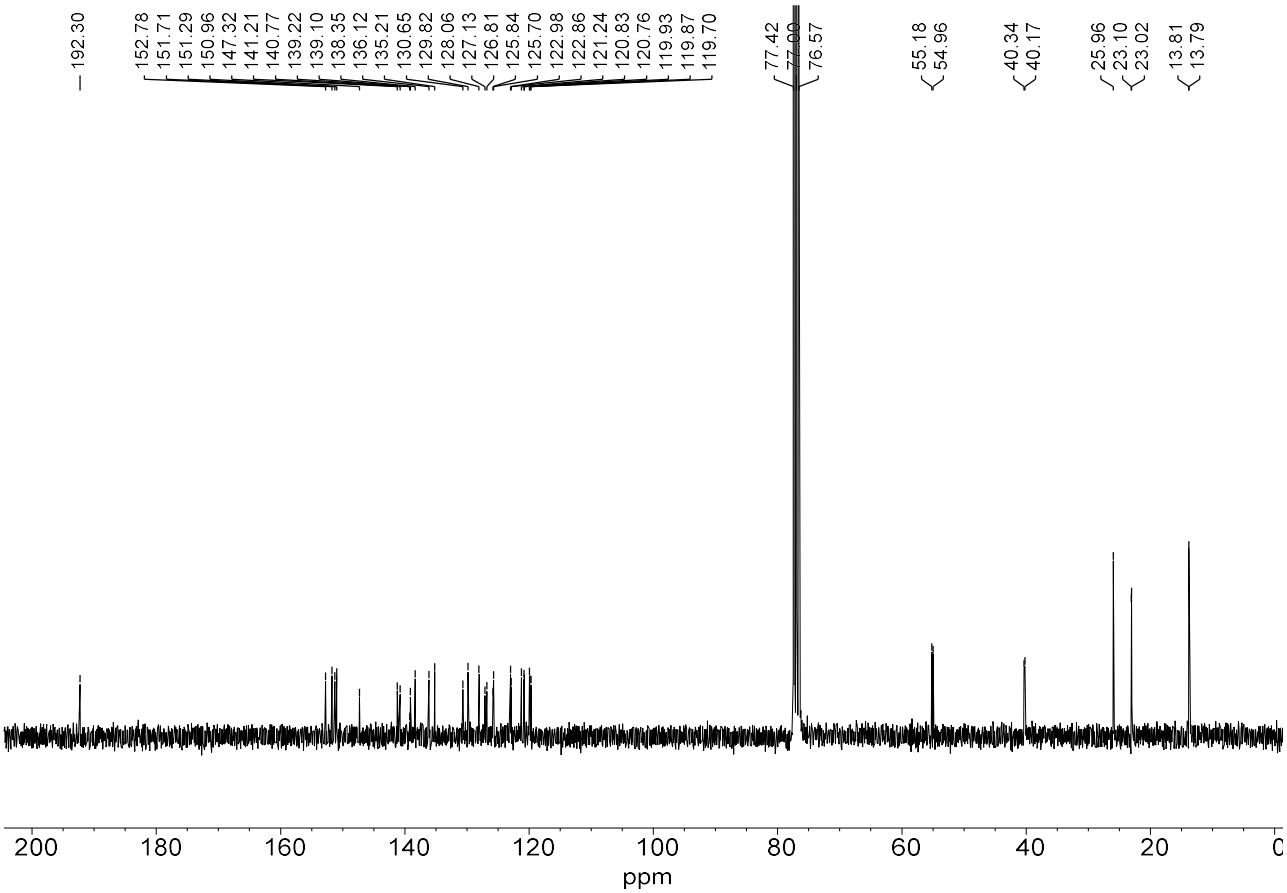

Figure S28. $^{13}C\{^{1}H\}$ NMR spectrum at 75 MHz for **10** in $CDCl_3$.

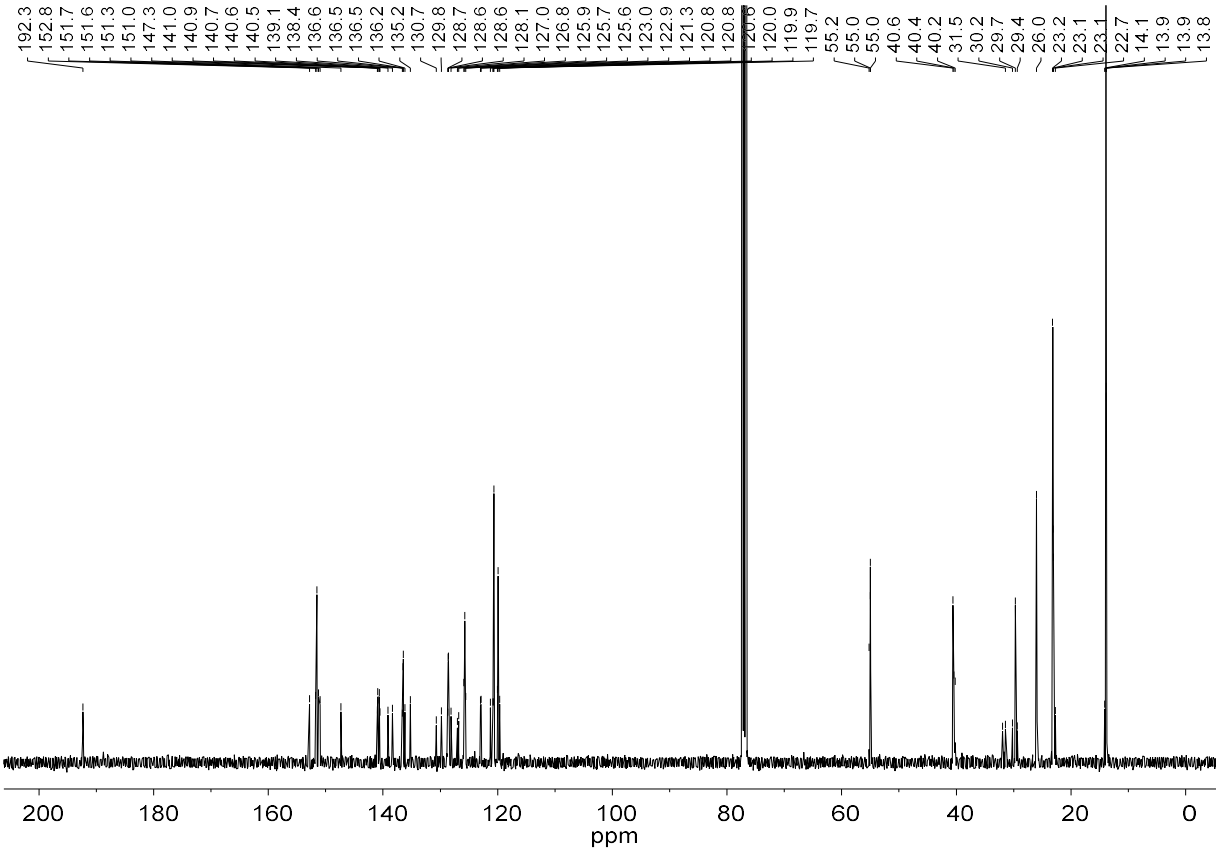

Figure S29. $^{13}C\{^{1}H\}$ NMR spectrum at 100 MHz for **11** in $CDCl_3$.

6. $^{13}C\{^1H\}$ NMR spectra for porphyrins 2a, 6b-e and 6b-d-Zn

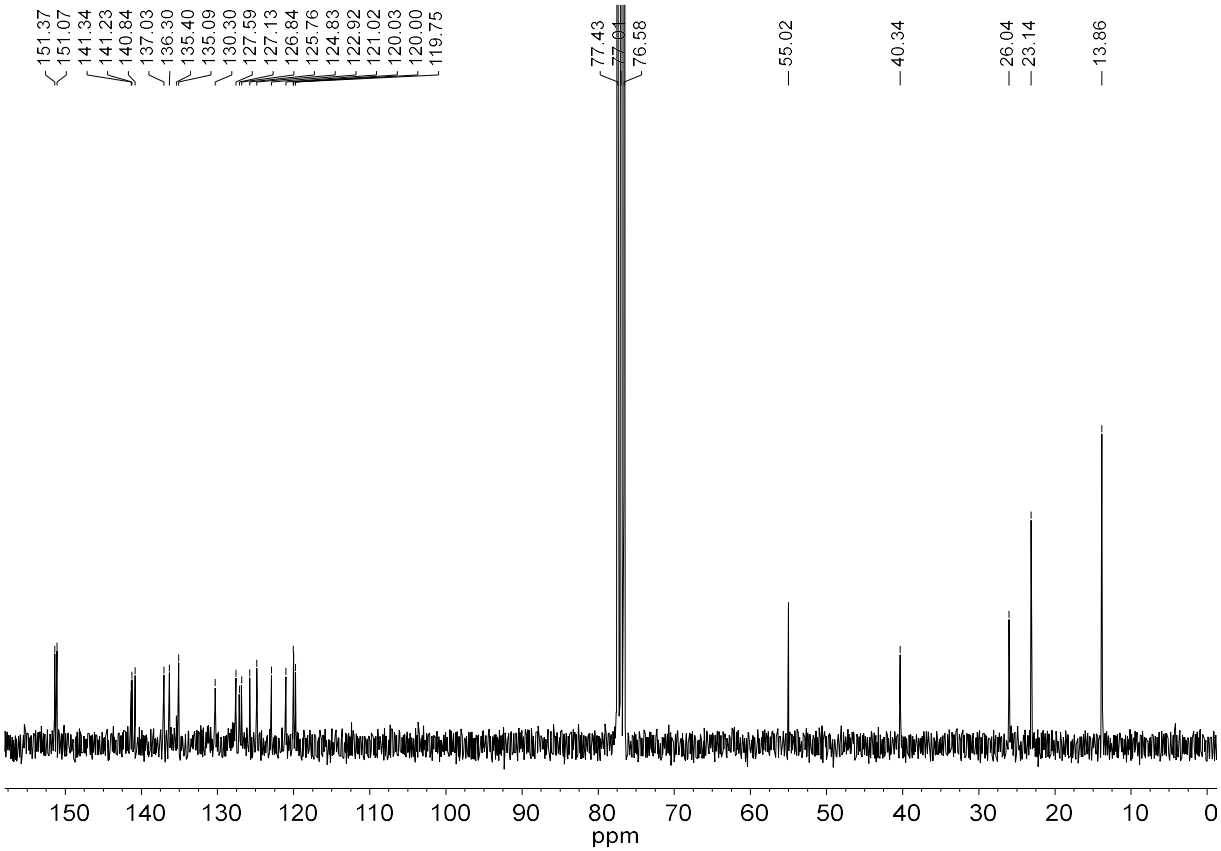

Figure S30. $^{13}C\{^1H\}$ NMR spectrum at 75 MHz for **2a** in $CDCl_3$.

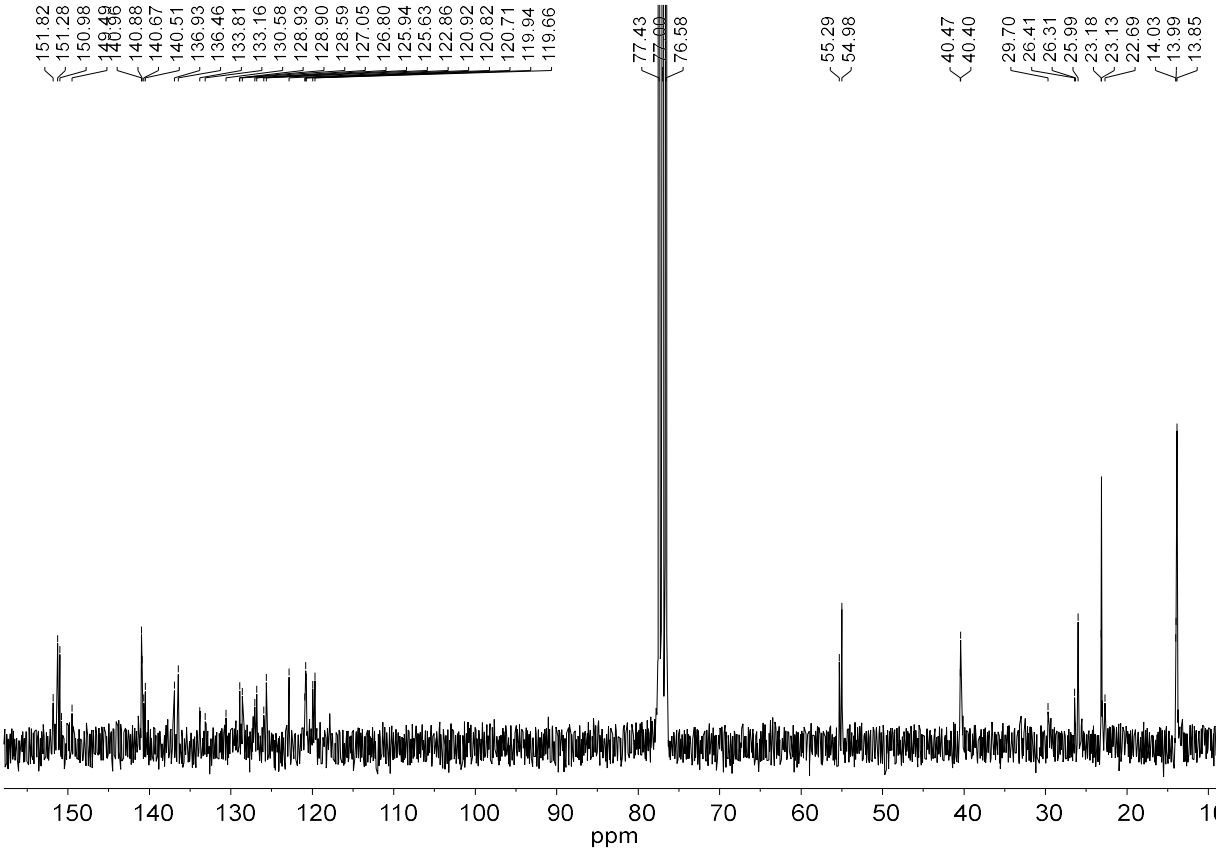

Figure S31. $^{13}C\{^{1}H\}$ NMR spectrum at 75 MHz for **6b** in $CDCl_3$.

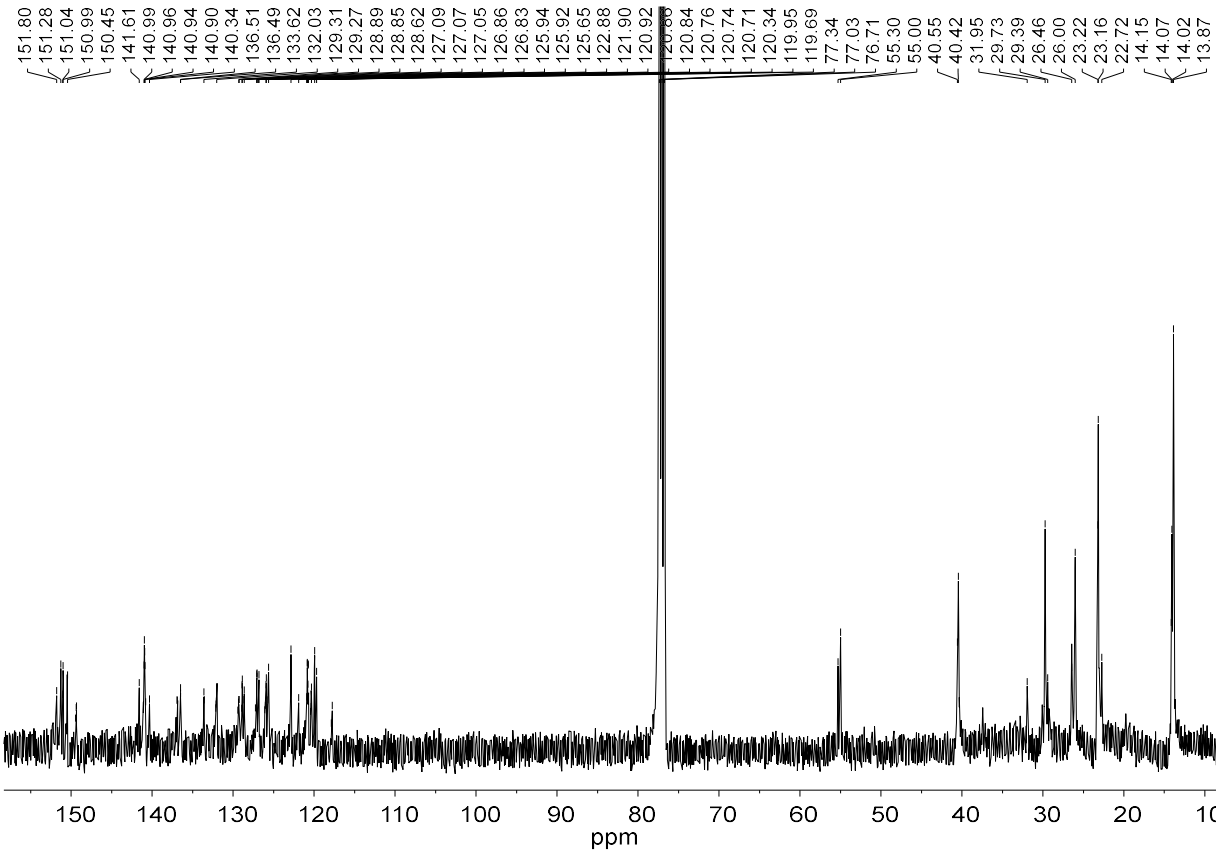

Figure S32. $^{13}C\{^{1}H\}$ NMR spectrum at 100 MHz for **6b-Zn** in $CDCl_3$.

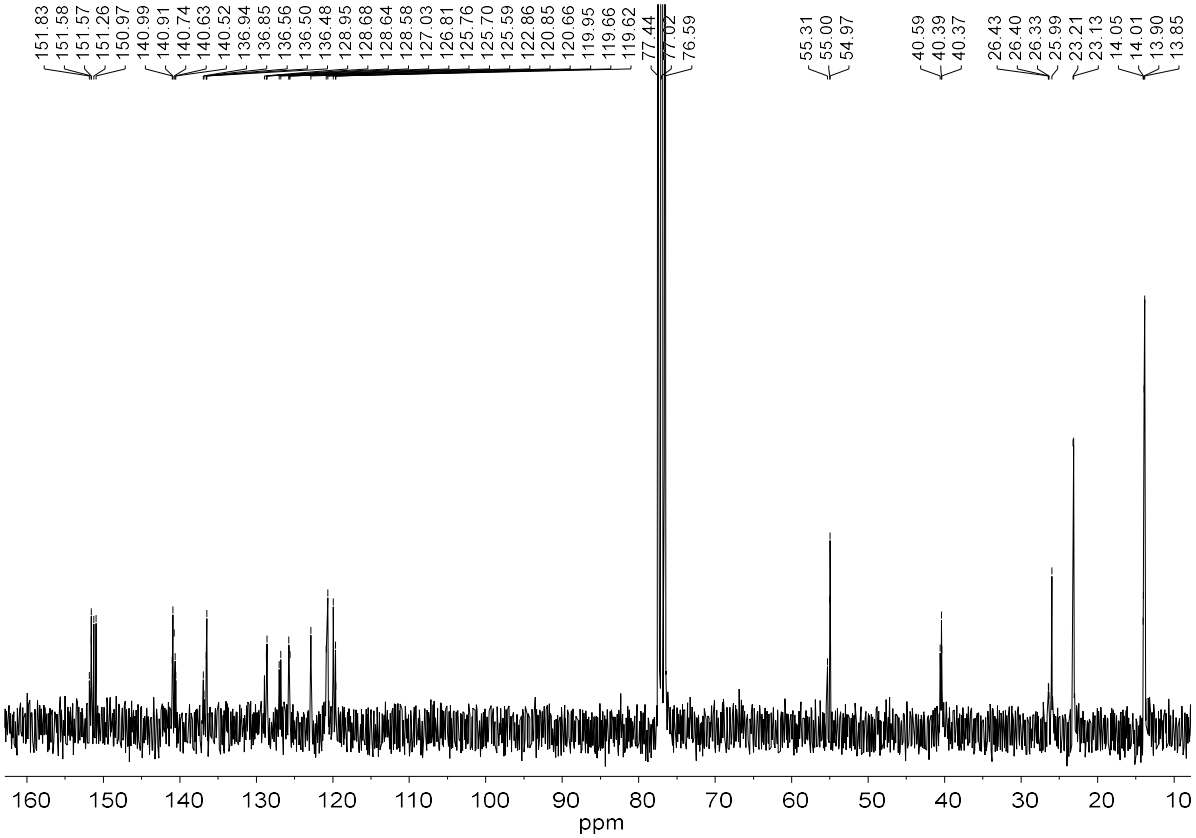

Figure S33. $^{13}C\{^{1}H\}$ NMR spectrum at 75 MHz for **6c** in $CDCl_3$.

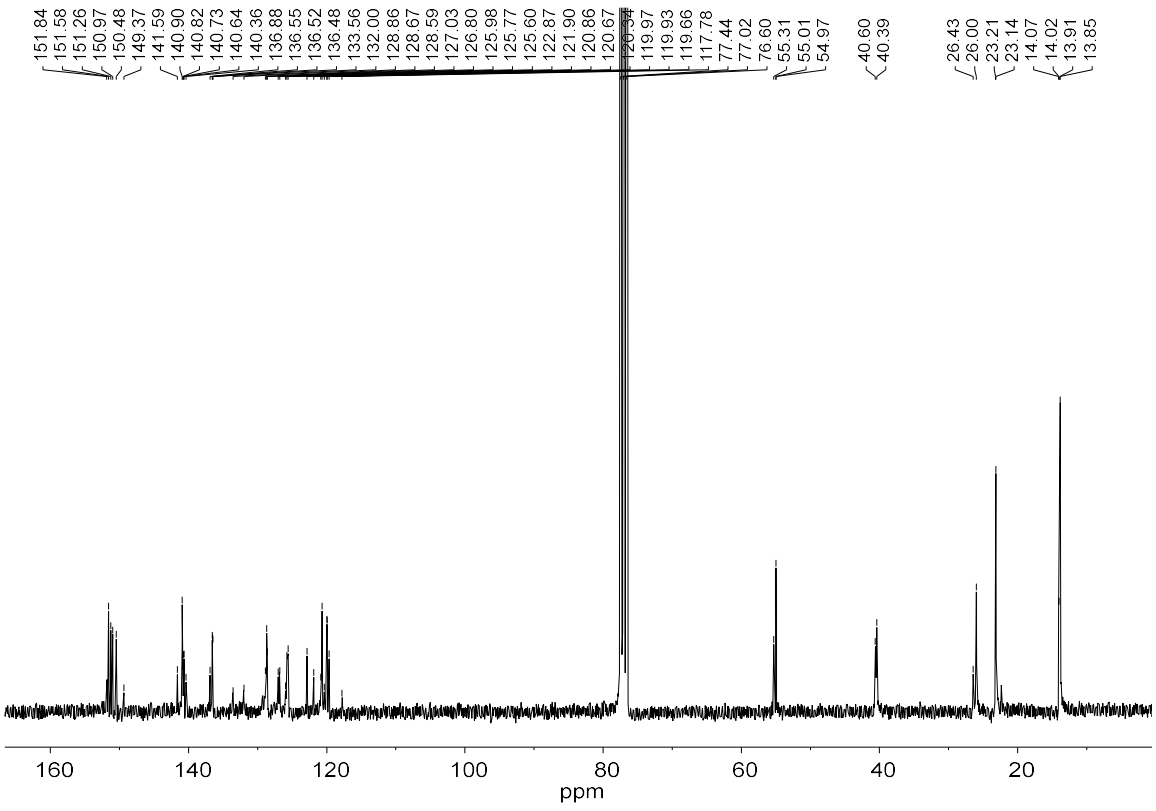

Figure S34. $^{13}C\{^{1}H\}$ NMR spectrum at 75 MHz for **6c-Zn** in $CDCl_3$.

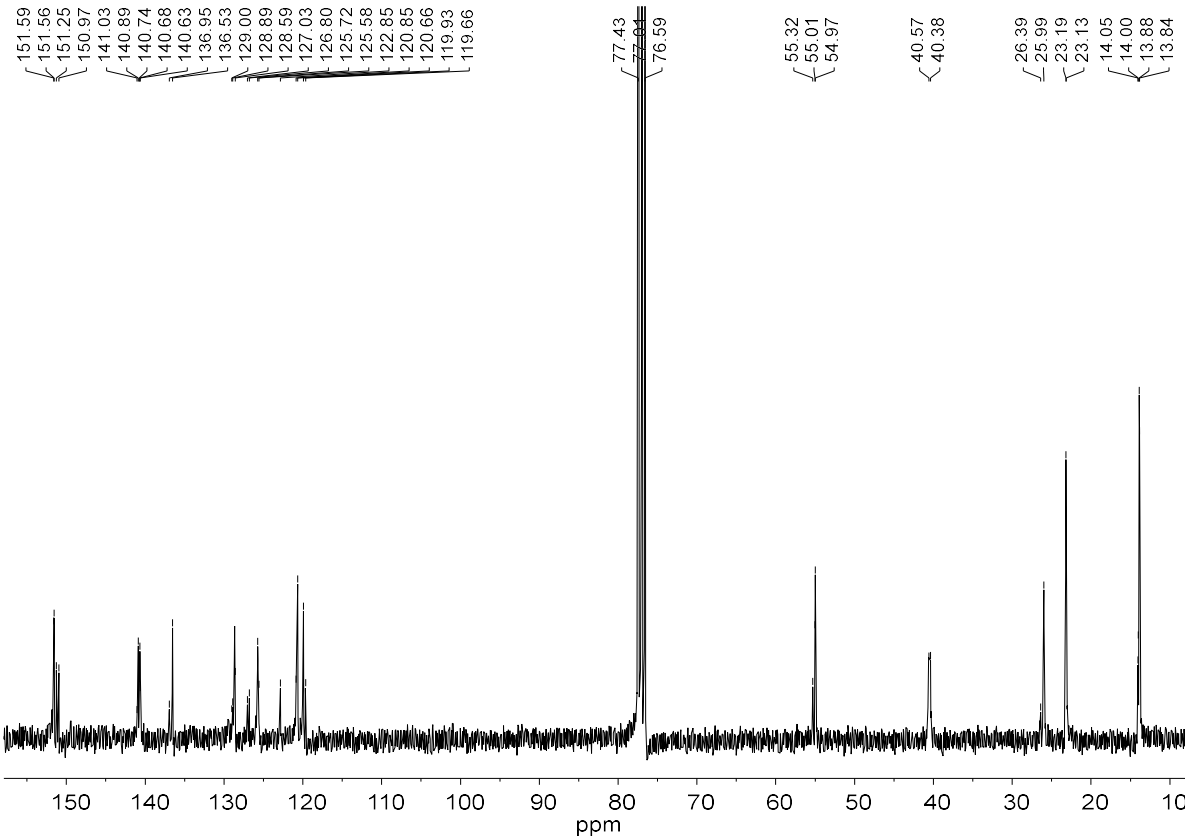

Figure S35. $^{13}C\{^{1}H\}$ NMR spectrum at 75 MHz for **6d** in $CDCl_3$.

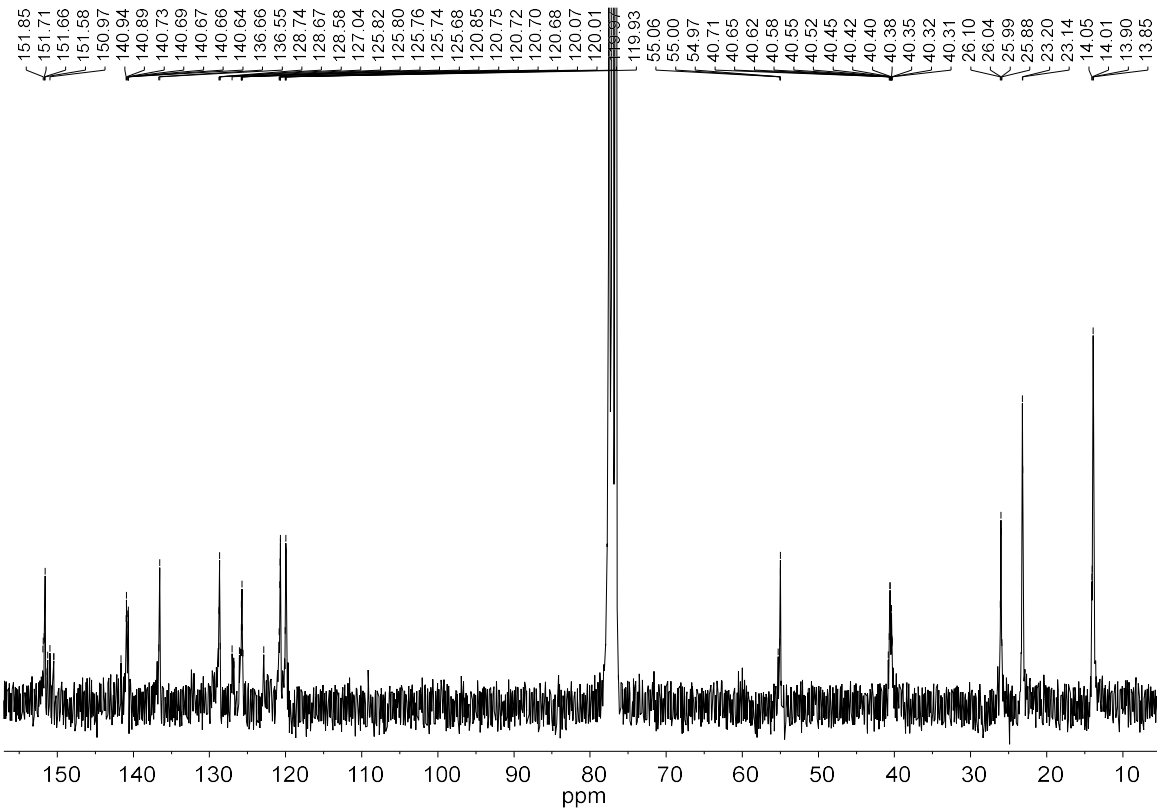

Figure S36. $^{13}C\{^{1}H\}$ NMR spectrum at 75 MHz for **6d-Zn** in $CDCl_3$.

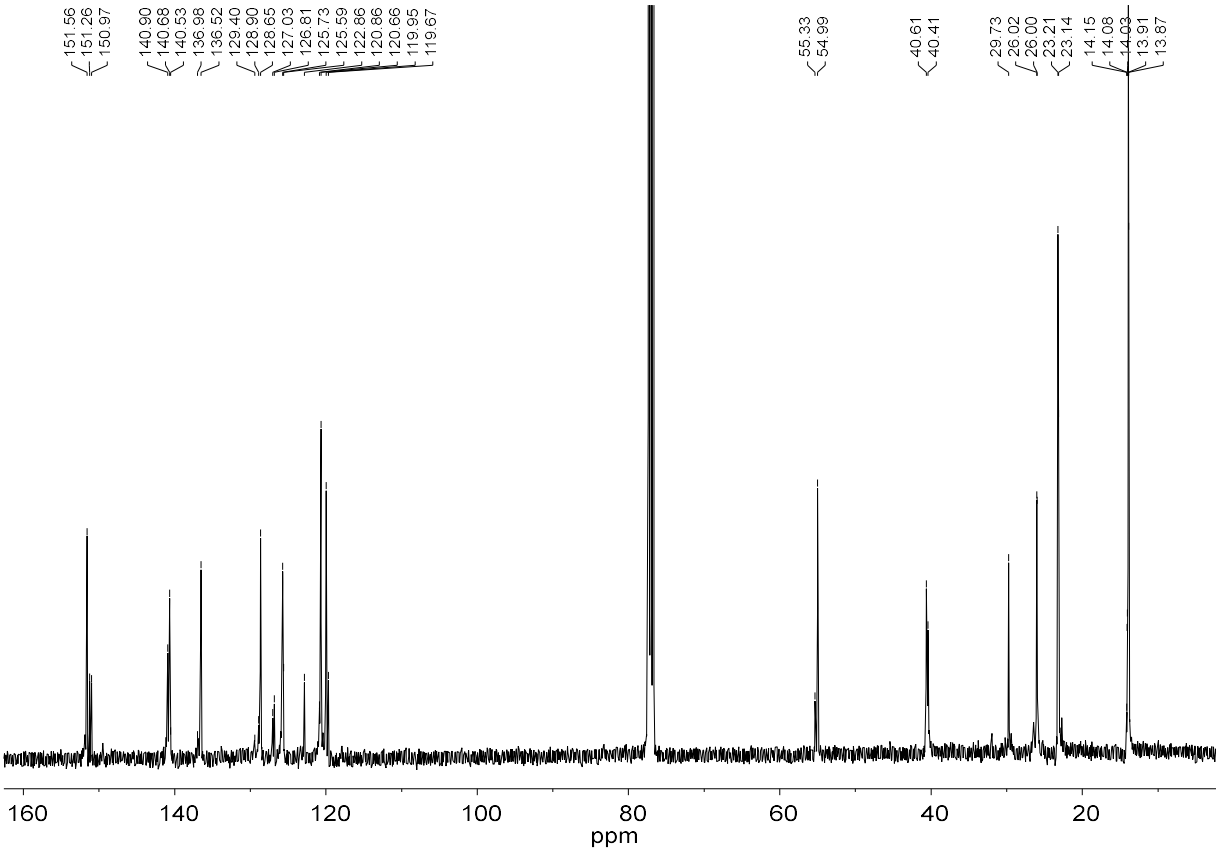

Figure S37. $^{13}C\{^{1}H\}$ NMR spectrum at 100 MHz for **6e** in $CDCl_3$.

7. Absorption and emission spectra of the aldehyde precursors 8-11

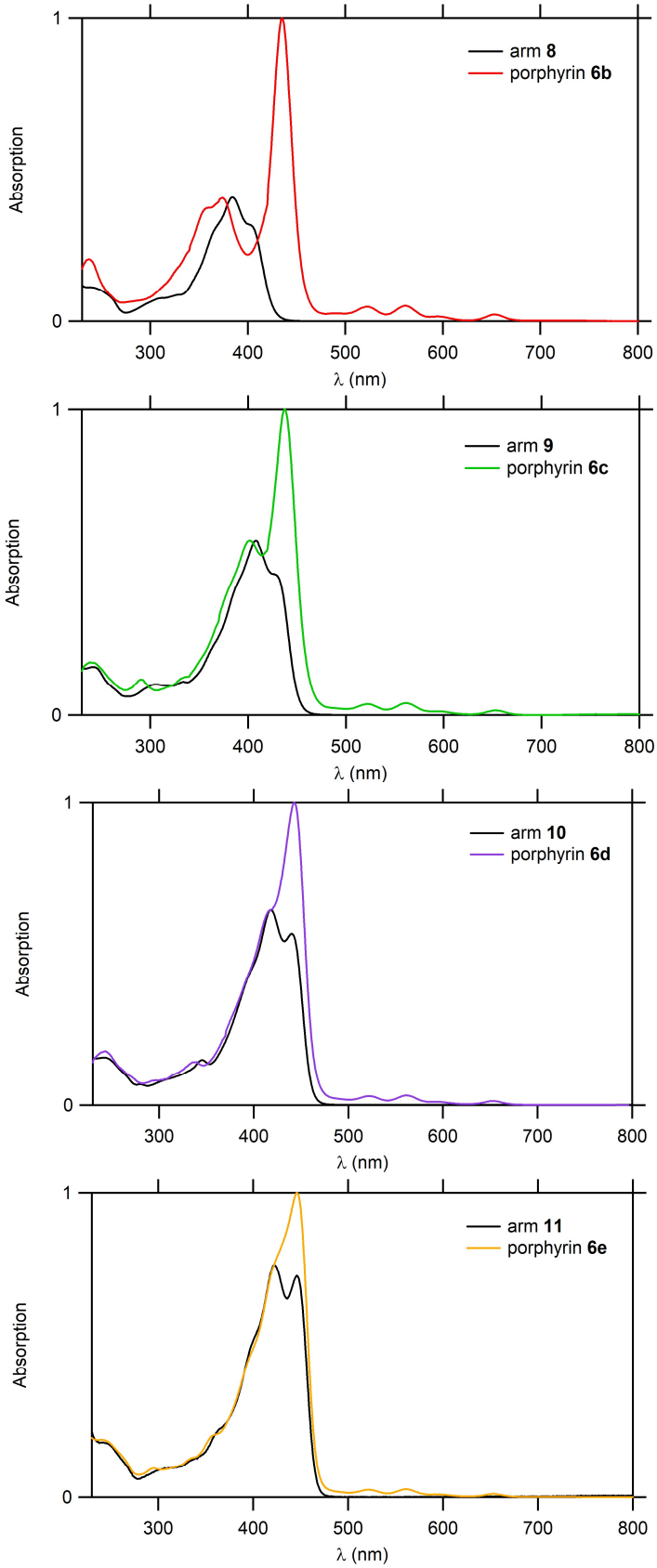

Figure S38. Comparison between the absorption spectra of porphyrins **6b-d** and the corresponding oligo-fluorenyl aldehydes **8-11**.

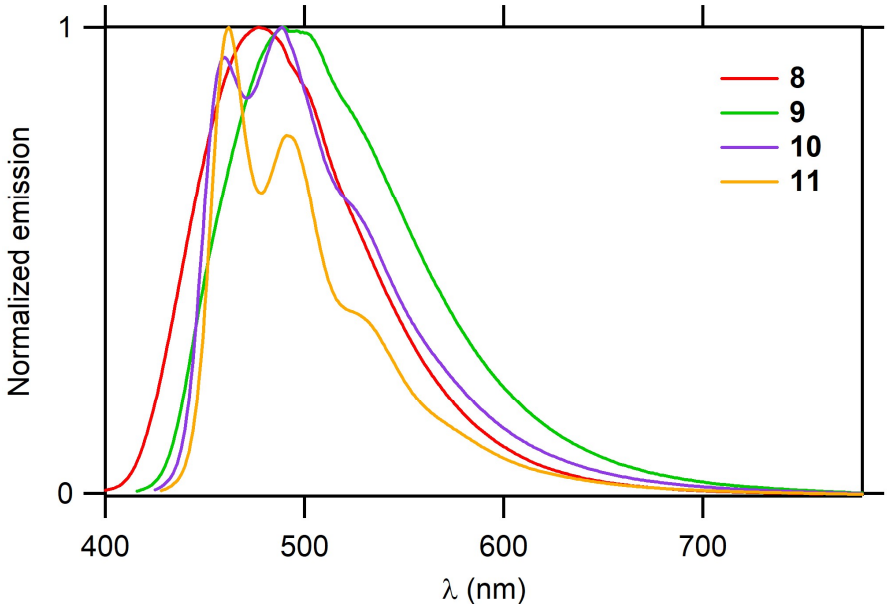

Figure S39. Normalized emission spectra of oligofluorenyl aldehydes **8-11** in CH_2Cl_2.

Table S1. Absorption and emission properties of oligofluorenyl aldehydes **8-11** in CH_2Cl_2.

Aldehyde	λ_{abs} (nm)	λ_{em} (nm)	Φ_F
8	383	477	0.98
9	408	490	0.94
10	418	460, 489, 524 (sh)	0.90
11	422	462, 491, 526 (sh)	0.93

8. Energy transfer efficiencies for 6b-e and 6b-d-Zn

The energy transfer efficiency (Φ_{EnT}) from oligo-fluorenyl arms (D) towards the central porphyrin core (A) in porphyrins **6b-e** and **6b-d-Zn** was estimated based on the decrease in donor fluorescence in dichloromethane. It is given by:

$$\Phi_{EnT} = 1 - \Phi_{DA} / \Phi_D^0$$

where Φ_{DA} is the fluorescence quantum yield of the donor in the presence of the acceptor (i.e. the fluorescence quantum yield of the oligo-fluorenyl arm in the presence of the porphyrin), and Φ_D^0 the fluorescence quantum yield of the donor in the absence of the acceptor (i.e. the fluorescence quantum yield of the arm model, in our case the aldehyde precursor).

Table S2. Energy transfer efficiencies for **6b-e** and **6b-d-Zn**.

Porphyrin	Donor model	Φ_{DA}	Φ_D^0	Φ_{EnT}
6b	**8**	0.005	0.98	0.99_5
6c	**9**	0.03	0.94	0.97
6d	**10**	0.009	0.90	0.99
6e	**11**	0.085	0.93	0.91
6b-Zn	**8**	0.025	0.98	0.97
6c-Zn	**9**	0.02	0.94	0.98
6d-Zn	**10**	0.023	0.90	0.97

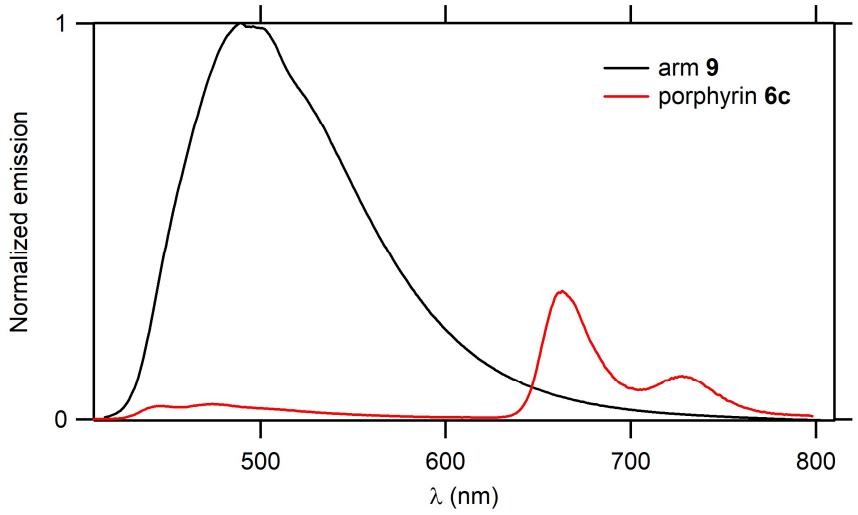

Figure S40. Example of donor (arm) fluorescence vs. porphyrin fluorescence (**9** vs. **6c)** in CH_2Cl_2.

9. Two-photon excited fluorescence (2PEF) data for 2a, 6b-e and 6b-d-Zn

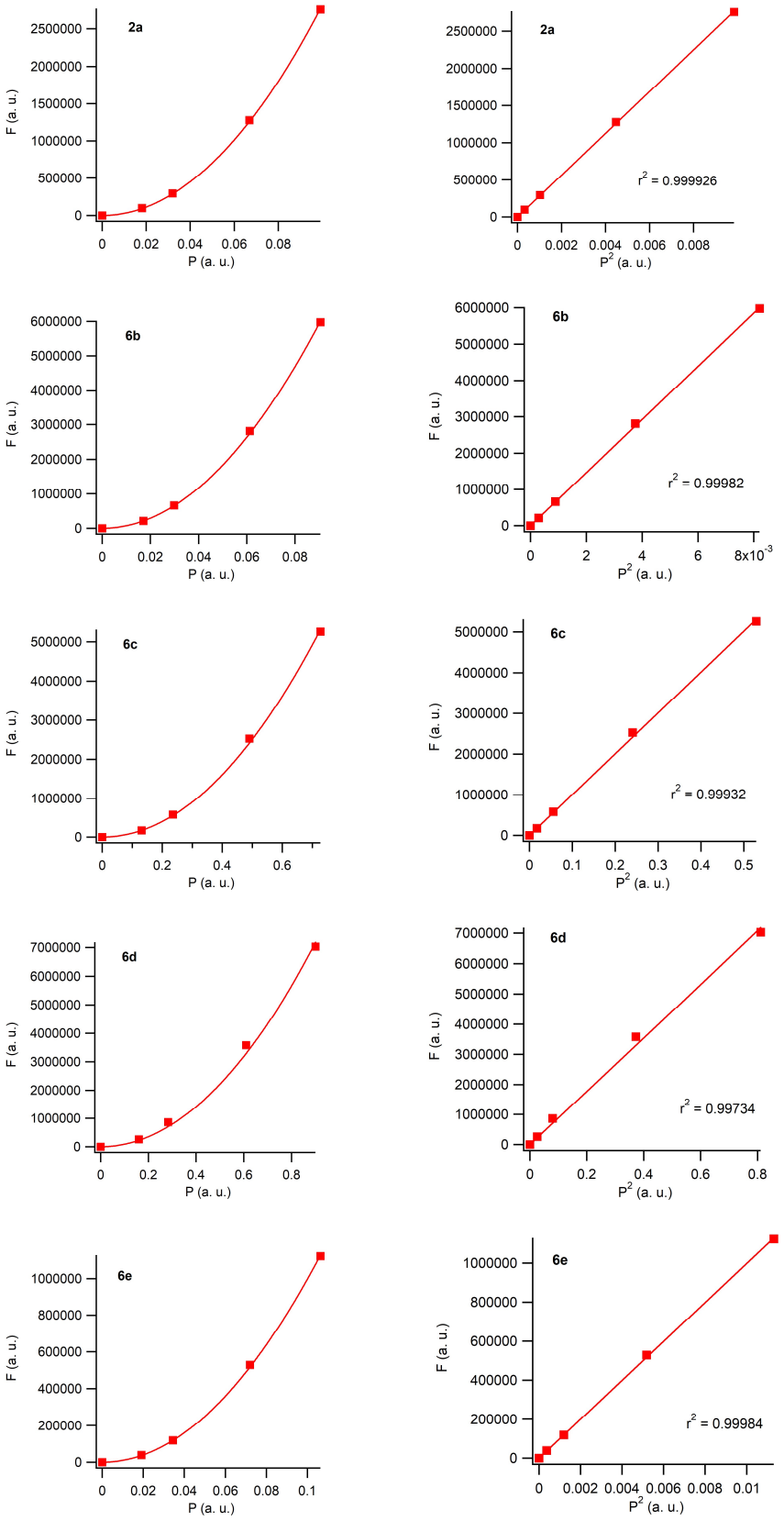

Figure S41. Left: quadratic dependence of the emission intensity (F) on laser excitation power (P) for compounds **2a**, **6b-e** at 790 nm. Right: dependence of F on P^2.

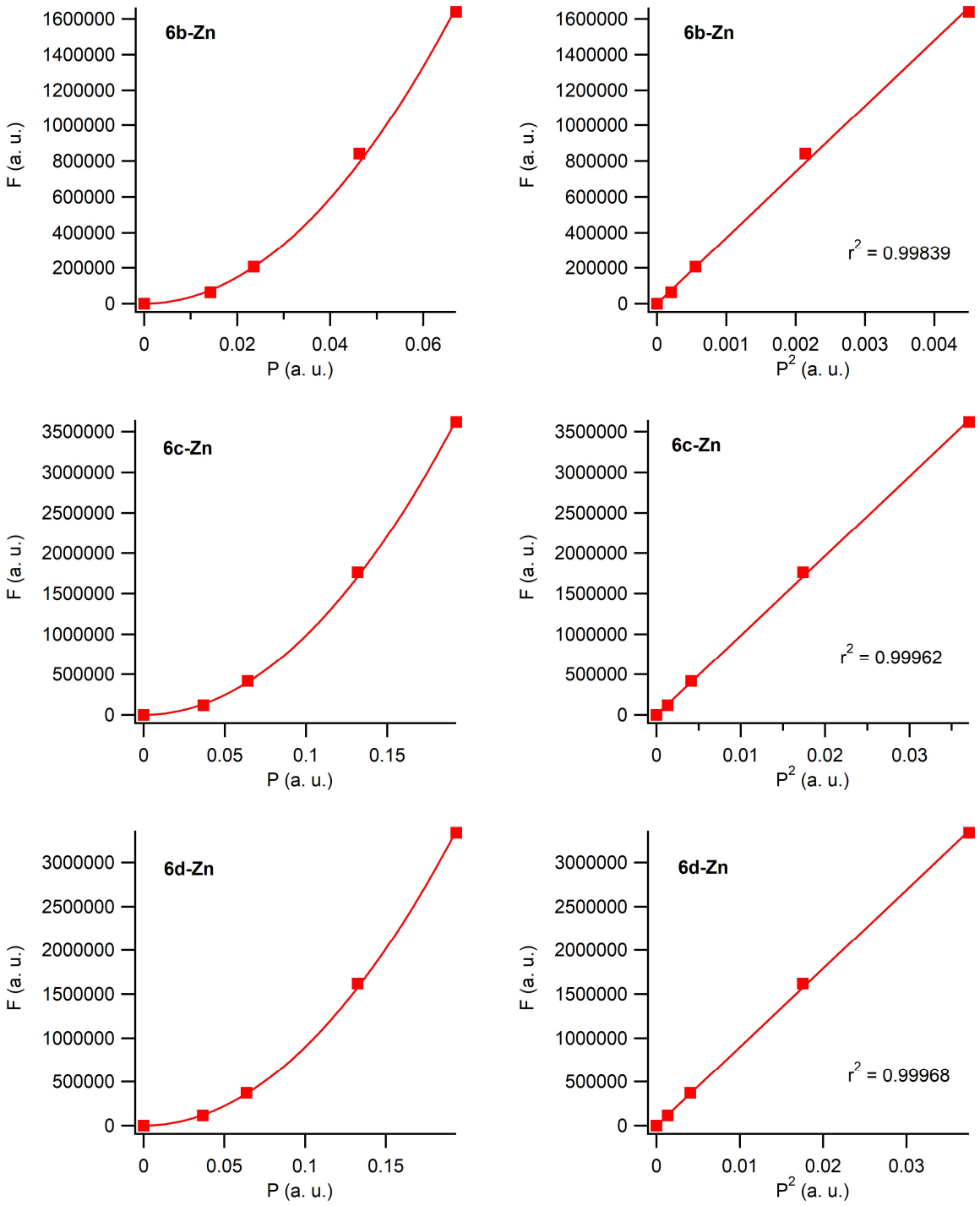

Figure S42. Left: quadratic dependence of the emission intensity (F) on laser excitation power (P) for compounds **6b-d-Zn** at 790 nm. Right: dependence of F on P^2.

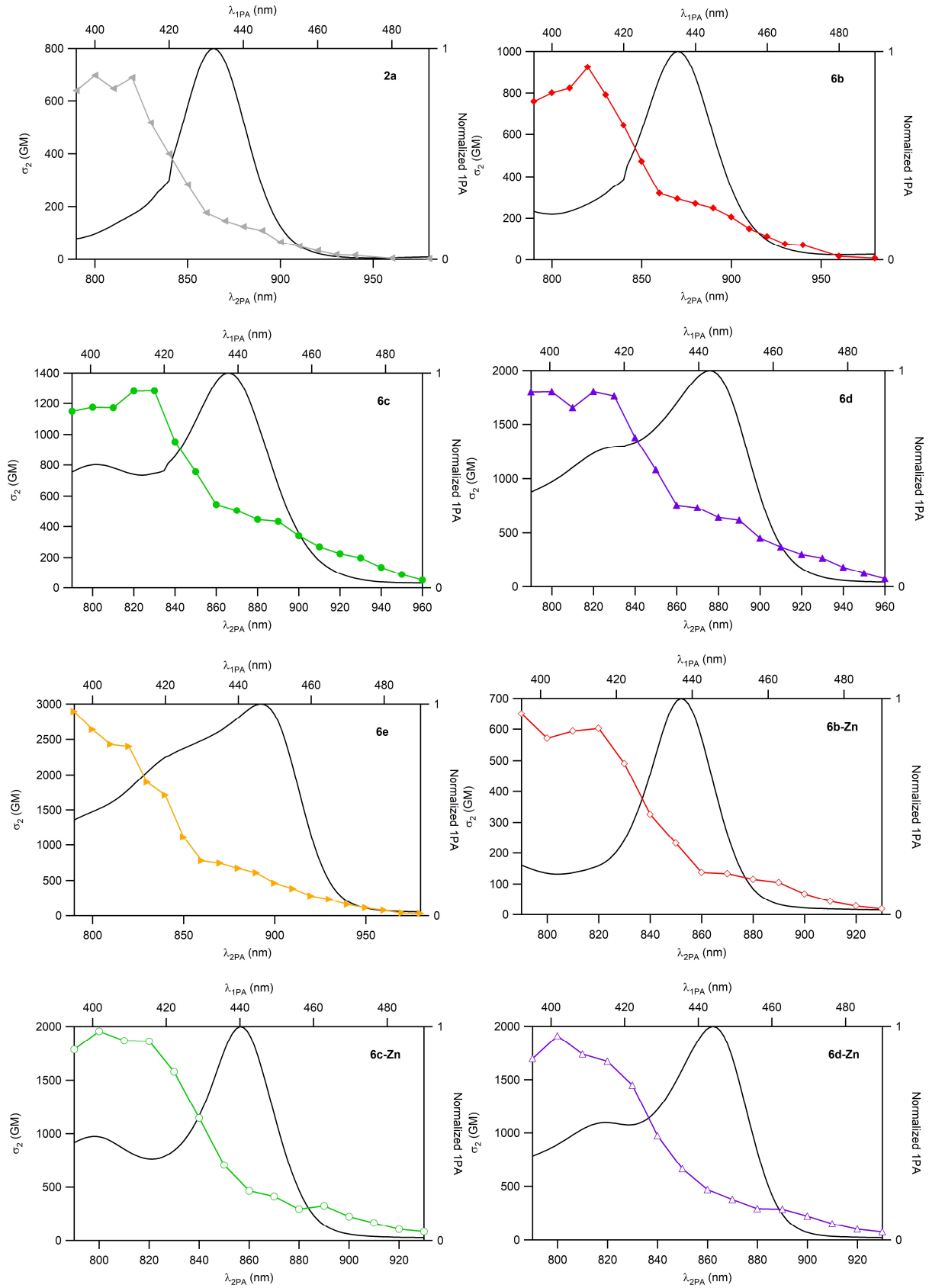

Figure S43. Overlay of one- and two-photon absorption spectra for compounds **2a**, **6b-e** and **6b-d-Zn** in CH_2Cl_2 (25 °C).